

Spring 2018

# OPTIMIZATION OF DRILLING AND BLASTING PRACTICES AT A WESTERN US OPEN PIT COPPER MINE

Joel Gadikor  
*Montana Tech*

Follow this and additional works at: [https://digitalcommons.mtech.edu/grad\\_rsch](https://digitalcommons.mtech.edu/grad_rsch)



Part of the [Mining Engineering Commons](#)

---

## Recommended Citation

Gadikor, Joel, "OPTIMIZATION OF DRILLING AND BLASTING PRACTICES AT A WESTERN US OPEN PIT COPPER MINE" (2018). *Graduate Theses & Non-Theses*. 168.  
[https://digitalcommons.mtech.edu/grad\\_rsch/168](https://digitalcommons.mtech.edu/grad_rsch/168)

This Thesis is brought to you for free and open access by the Student Scholarship at Digital Commons @ Montana Tech. It has been accepted for inclusion in Graduate Theses & Non-Theses by an authorized administrator of Digital Commons @ Montana Tech. For more information, please contact [sjuskiewicz@mtech.edu](mailto:sjuskiewicz@mtech.edu).

OPTIMIZATION OF DRILLING AND BLASTING PRACTICES AT A  
WESTERN US OPEN PIT COPPER MINE

by

Joel Edem Kwaku Gadikor

A thesis submitted in partial fulfillment of the  
requirements for the degree of

Master of Science in Mining Engineering

Montana Tech

2018



## Abstract

The mining process begins with drilling and blasting activities. The efficiency of blasting affects all downstream operations such as loading, hauling, crushing and milling. Therefore drilling and blasting activities should be designed to ensure that designed parameters produce the desired fragmentation. The Kuz-Ram model is a fragmentation prediction model and is widely used for predicting the fragmentation distribution from blasting in the mining industry. This research evaluates the performance of the Kuz-Ram and Modified Kuz-Ram models to determine the most accurate models applicable to a Western US open pit copper mine's fragmentation data. The performance assessment was done using the Root Mean Square Error and correlation and regression analyses. A general trend of under estimation of the fines ( $< 0.75$  inch) and over estimation of oversize ( $\geq 25$  inch) was observed using the Kuz-Ram and Modified Kuz-Ram models as compared to the Split image analysis obtained in the field. From the image analysis, the average actual amount of fines produced from the eight blasts studied was 27.62% with an insignificant amount of oversize material less than 5%. Though all the models had high correlation coefficient, R and coefficient of determination,  $R^2$  values (above 95%) in predicting the fragmentation distribution, the Modified Kuz-Ram model performed well in six out of the eight blasts considered while the Kuz-Ram model performed best in two out of the eight blasts considered.

Keywords: Drilling, blasting, open pit, fragmentation, Kuz-Ram model, Modified Kuz-Ram model

## **Dedication**

This project work is dedicated to my dear parents, Mr. Joseph Newton Kwaku Gadikor and Mrs. Vivian Kafui Gadikor and the entire Gadikor and Mortoti families.

## **Acknowledgements**

My sincere gratitude, first and foremost, goes to the Almighty God for his protection and grace that have sustained me this far. I would also like to thank Montana Tech for their financial support over my entire two years of my master's program. Without their financial support, I would not have been able to maintain my status as a full-time student, let alone complete this degree in a timely manner.

Thank you to my graduate committee members: Scott Rosenthal, Chris Roos and Dr. Das Avimanyu for your helpful suggestions during this process and has given my work great meaning.

A special thanks to Scott Rosenthal, my committee chair and advisor, for your guidance and ability to keep me on track with this project. And to my family members who have always been my source of inspiration and helped me in all my decision making, I say may God continue to hold us as one people and may their investment in me yield bountifully.

## Table of Contents

<b>ABSTRACT .....</b>	<b>II</b>
<b>DEDICATION .....</b>	<b>III</b>
<b>ACKNOWLEDGEMENTS .....</b>	<b>IV</b>
<b>LIST OF TABLES .....</b>	<b>IX</b>
<b>LIST OF FIGURES.....</b>	<b>XI</b>
<b>LIST OF EQUATIONS .....</b>	<b>XIII</b>
1. INTRODUCTION .....	1
1.1. <i>Project Objectives</i> .....	2
2. LITERATURE REVIEW.....	3
2.1. <i>Drilling</i> .....	3
2.2. <i>Blasting</i> .....	3
2.3. <i>Bench Blasting</i> .....	4
2.4. <i>Uncontrollable Factors</i> .....	5
2.4.1. Rock Geotechnical Properties .....	5
2.4.1.1. Rock Strength.....	5
2.4.1.2. Elasticity .....	7
2.4.1.3. Density .....	7
2.4.1.4. Porosity .....	7
2.4.2. Rock Structure .....	8
2.5. <i>Controllable Factors</i> .....	8
2.5.1. Geometrical Parameters .....	9
2.5.1.1. Hole Diameter .....	9
2.5.1.2. Sub drill Depth .....	9
2.5.1.3. Bench Height.....	10
2.5.1.4. Stemming Height and Material .....	10

2.5.1.5.	Burden.....	11
2.5.1.6.	Spacing.....	12
2.5.2.	Explosive Factors.....	12
2.5.2.1.	Powder Factor.....	13
2.5.2.2.	Type and Properties of Explosives.....	13
2.6.	<i>Fragmentation Analysis</i> .....	14
2.6.1.	Split-Desktop® Software.....	14
2.6.1.1.	Image Acquisition and Scaling.....	16
2.6.1.2.	Fragment Delineation.....	19
2.6.1.3.	Editing of Delineated Image.....	19
2.6.1.4.	Calculation of the Size Distribution.....	20
2.6.1.5.	Presentation of the Size Distribution Results.....	21
2.7.	<i>Fragmentation Modelling/Prediction</i> .....	22
2.7.1.	Kuz-Ram Model.....	23
2.7.1.1.	Kuznetsov's Equation.....	23
2.7.1.2.	Rosin-Rammler's Equation.....	24
2.7.1.3.	Cunningham's Uniformity index.....	24
2.7.2.	Modified Kuz-Ram Model.....	26
2.8.	<i>Statistical Analysis</i> .....	28
2.8.1.	Root Mean Square Error Method.....	28
2.8.2.	Regression and Correlation.....	29
3.	DATA COLLECTION AND ANALYSIS.....	30
3.1.	<i>Introduction</i> .....	30
3.2.	<i>Data Collection</i> .....	30
3.2.1.	Geometric Blast Design Data.....	30
3.2.2.	Explosives Data.....	31
3.2.3.	Rock Parameters.....	31
3.2.4.	Muckpile Image Sampling.....	32
3.3.	<i>Data Analysis</i> .....	33

4. RESULTS AND DISCUSSIONS.....	37
4.1. Introduction.....	37
4.2. Fragmentation Analysis .....	37
4.2.1. Blast #3053 .....	37
4.2.2. Blast #3054 .....	38
4.2.3. Blast #3056 .....	39
4.2.4. Blast #3060 .....	39
4.2.5. Blast #3062 .....	40
4.2.6. Blast #3063 .....	41
4.2.7. Blast #3065 .....	41
4.2.8. Blast #3067 .....	42
4.3. Fragmentation Prediction .....	44
4.3.1. Blast #3053 .....	44
4.3.2. Blast #3054 .....	46
4.3.3. Blast #3056 .....	47
4.3.4. Blast #3060 .....	49
4.3.5. Blast #3062 .....	50
4.3.6. Blast #3063 .....	52
4.3.7. Blast #3065 .....	53
4.3.8. Blast #3067 .....	55
4.4. Determination of Model Performance .....	57
4.5. Model Comparison Discussion .....	59
5. CONCLUSION AND RECOMMENDATION .....	60
5.1. Conclusion .....	60
5.2. Recommendations .....	61
6. REFERENCES CITED.....	62
7. APPENDIX A: ACTUAL FRAGMENTATION DISTRIBUTION AND PREDICTIVE MODELS RESULTS .....	65
8. APPENDIX B: ROOT MEAN SQUARE ERROR RESULTS FOR THE PREDICTIVE MODELS .....	73

9. APPENDIX C: CORRELATION AND REGRESSION ANALYSIS RESULTS. .... 81

## List of Tables

Table I: Engineering classification of rock by compressive strength, Marinos & Hoek (2001). .....	6
Table II: Effect of blasting parameters on Uniformity Index (n), Cunningham (1983). ...	26
Table III: Geometric Blast Parameters at Continental Pit .....	30
Table IV: Explosive Parameters of Blasts at Continental Pit .....	31
Table V: Summary of Rock Parameters at Continental Pit .....	32
Table VI: Summary of Fragmentation Analysis Results for Blasts at Continental Pit.....	43
Table VII: Fragmentation Prediction Summary for Blast #3050.....	45
Table VIII: Fragmentation Prediction Summary for Blast #3054 .....	47
Table IX: Fragmentation Prediction Summary for Blast #3056.....	49
Table X: Fragmentation Prediction Summary for Blast #3060 .....	50
Table XI: Fragmentation Prediction Summary for Blast #3062.....	52
Table XII: Fragmentation Prediction Summary for Blast #3063.....	53
Table XIII: Fragmentation Prediction Summary for Blast #3065 .....	55
Table XIV: Fragmentation Prediction Summary for Blast #3067 .....	56
Table XV: Summary of Predicted Mean Fragment Sizes for the Blasts .....	57
Table XVI: Summary of the Estimated RMSE of the Models .....	58
Table XVII: Summary of Correlation and Regression Analysis Results for the Models..	58
Table XVIII: Size Distribution Results for Blast #3053.....	65
Table XIX: Size Distribution Results for Blast #3054. ....	66
Table XX: Size Distribution Results for Blast #3056.....	67
Table XXI: Size Distribution Results for Blast #3060. ....	68

Table XXII: Size Distribution Results for Blast #3062.....	69
Table XXIII: Size Distribution Results for Blast #3063.....	70
Table XXIV: Size Distribution Results for Blast #3065. ....	71
Table XXV: Size Distribution Results for Blast #3067.....	72
Table XXVI: RMSE results for Blast #3053. ....	73
Table XXVII: RMSE results for Blast #3054.....	74
Table XXVIII: RMSE results for Blast #3056. ....	75
Table XXIX: RMSE results for Blast #3060. ....	76
Table XXX: RMSE results for Blast #3062. ....	77
Table XXXI: RMSE results for Blast #3063. ....	78
Table XXXII: RMSE results for Blast #3065.....	79
Table XXXIII: RMSE results for Blast #3067. ....	80

## List of Figures

Figure 1: Bench blast geometry and terminology (Onlineminingexam, 2018). .....	4
Figure 2: A large scale muckpile image. ....	17
Figure 3: A medium scale muckpile image. ....	18
Figure 4: A small scale muckpile image.....	18
Figure 5: Delineation of the muckpile image with masked scale balls (light blue) and fines fill (red).....	20
Figure 6: Log-Linear Size distribution plot result. ....	21
Figure 7: Rock Parameters Description and Ratings (Source: Lilly 1986). ....	25
Figure 8: Delineated muckpile image.....	34
Figure 9: Kuz-Ram and Modified Kuz-Ram models in MS Excel 2016.....	35
Figure 10: Fragmentation Size Distribution for Blast #3053.....	38
Figure 11: Fragmentation Size Distribution for Blast #3054.....	38
Figure 12: Fragmentation Size Distribution for Blast #3056.....	39
Figure 13: Fragmentation Size Distribution for Blast #3060.....	40
Figure 14: Fragmentation Size Distribution for Blast #3062.....	40
Figure 15: Fragmentation Size Distribution for Blast #3063.....	41
Figure 16: Fragmentation Size Distribution for Blast #3065.....	42
Figure 17: Fragmentation Size Distribution for Blast #3067.....	43
Figure 18: Actual Size Distribution against Predictive Models for Blast #3053.....	45
Figure 19: Actual Size Distribution against Predictive Models for Blast #3054.....	47
Figure 20: Actual Size Distribution against Predictive Models for Blast #3056.....	48
Figure 21: Actual Size Distribution against Predictive Models for Blast #3060.....	50

Figure 22: Actual Size Distribution against Predictive Models for Blast #3062.....	51
Figure 23: Actual Size Distribution against Predictive Models for Blast #3063.....	53
Figure 24: Actual Size Distribution against Predictive Models for Blast #3065.....	54
Figure 25: Actual Size Distribution against Predictive Models for Blast #3067.....	56
Figure 26: Correlation between Actual Predicted Fragmentation Results for Blast #3053.	81
Figure 27: Correlation between Actual Predicted Fragmentation Results for Blast #3054.	82
Figure 28: Correlation between Actual Predicted Fragmentation Results for Blast #3056.	83
Figure 29: Correlation between Actual Predicted Fragmentation Results for Blast #3060.	84
Figure 30: Correlation between Actual Predicted Fragmentation Results for Blast #3062.	85
Figure 31: Correlation between Actual Predicted Fragmentation Results for Blast #3063.	86
Figure 32: Correlation between Actual Predicted Fragmentation Results for Blast #3065.	87
Figure 33: Correlation between Actual Predicted Fragmentation Results for Blast #3067.	88

**List of Equations**

Equation (1) .....	9
Equation (2) .....	10
Equation (3) .....	11
Equation (4) .....	13
Equation (5) .....	24
Equation (6) .....	24
Equation (7) .....	24
Equation (8) .....	25
Equation (9) .....	25
Equation (10) .....	27
Equation (11) .....	27
Equation (12) .....	27
Equation (13) .....	27
Equation (14) .....	28
Equation (15) .....	28
Equation (16) .....	28

## 1. Introduction

The mining process begins with drilling and blasting activities, and these unit operations have a significant impact on downstream processes such as loading, hauling, crushing and milling.

Drilling and blasting are seen as sub-systems of the size reducing operations in mining. To have better design parameters for economical excavation of mineral production and good fragmentation, the drilling and blasting operations needs to be optimized to improve fragmentation, which in turn will have a positive impact on the diggability of the material, reducing the time and energy to load. Better fragmentation sizes, meaning producing more fines, will reduce the energy required to crush and grind the material hence increasing crusher and mill throughput. Other benefits include improving the conditions of the bench floor, reducing flyrock, reducing ground vibrations and reduce secondary blasting. In mining, the rock fragments obtained from blasting are usually further processed to liberate the minerals of interest or to attain the appropriate end use fragment sizes. The characteristics of these fragments are very important as they affect the overall efficiency of the downstream processes including loading, hauling and processing. It is therefore important that much attention is given to blast design. This can be done by using the available fragmentation prediction models to predict the fragmentation distribution that results from using a particular set of blasting parameters and hence selecting those that give the required fragmentation.

There is therefore the need to use fragmentation models to establish their applicability to surface blast designs by comparing prediction results with field results to determine their accuracy. This research therefore seeks to study the performance of the Kuz-Ram and Modified Kuz-Ram models to fragmentation prediction at a Western US open pit copper mine.

## 1.1. Project Objectives

The main objectives of this project are:

- Analyze the actual size distribution of the resulting muckpile from the various blasts using Split-Desktop® Image Analysis Software;
- Develop fragmentation models to predict the fragmentation distribution using the designed drilling and blasting parameters at the mine;
- Determine the performance of the models by comparing the predictive results to the actual fragmentation results obtained from the Image Analysis technique using statistical methods; and,
- Recommend measures and strategies to improve both the drilling and blasting practices at the mine.

## **2. Literature Review**

The literature review focused on topics of drilling and blasting in the mining industry pertaining to drilling, blasting, fragmentation analysis techniques using predictive models and image analysis techniques.

### **2.1. Drilling**

Drilling is the process of making a hole into a hard surface where the length of the hole is very large compared to the diameter (Pathak, 2014). Drilling and Blasting is the most common method for breaking and loosening solid rock in surface mines. The general objective is to produce the broken material that can be excavated and loaded.

Surface mining requires drilling for different purposes that include (Pathak, 2014):

- Production drilling i.e. for making holes for placement of explosives for blasting.
- Exploration drilling i.e. for sample collections to estimate the quality and quantity of a mineral reserve.
- Technical drilling i.e. during development of a mine for drainage, slope stability and foundation testing purposes.

### **2.2. Blasting**

Blasting is the process of fracturing material by the use of a calculated amount of explosive so that a predetermined volume of material is broken (Phifer & Hem, 2012). Good blast design and execution are essential to successful mining operations. Improper or poor practices in blasting can have a severely negative impact on the economics of a mine. Examples of explosives used in blasting in surface mines include ANFO (ammonium nitrate/fuel oil), Slurries and Emulsions. Many factors are taken into account when determining what type of

blast design or explosive will be used. Rock type, density and strength are all important factors, as well as fracture condition of the rock, cost and water conditions.

### 2.3. Bench Blasting

Achieving a well-distributed particle size is the main goal of blasting, so that the rock can be handled efficiently in post-blast processes, e.g. loading and crushing. The outcome of a blast is influenced by several parameters; mechanical properties of rock mass, geometry of blast holes, type and amount of explosives, initiation pattern and delay times are some of the key factors in blast design. A brief terminology of bench blasting geometry is presented in Figure 1.

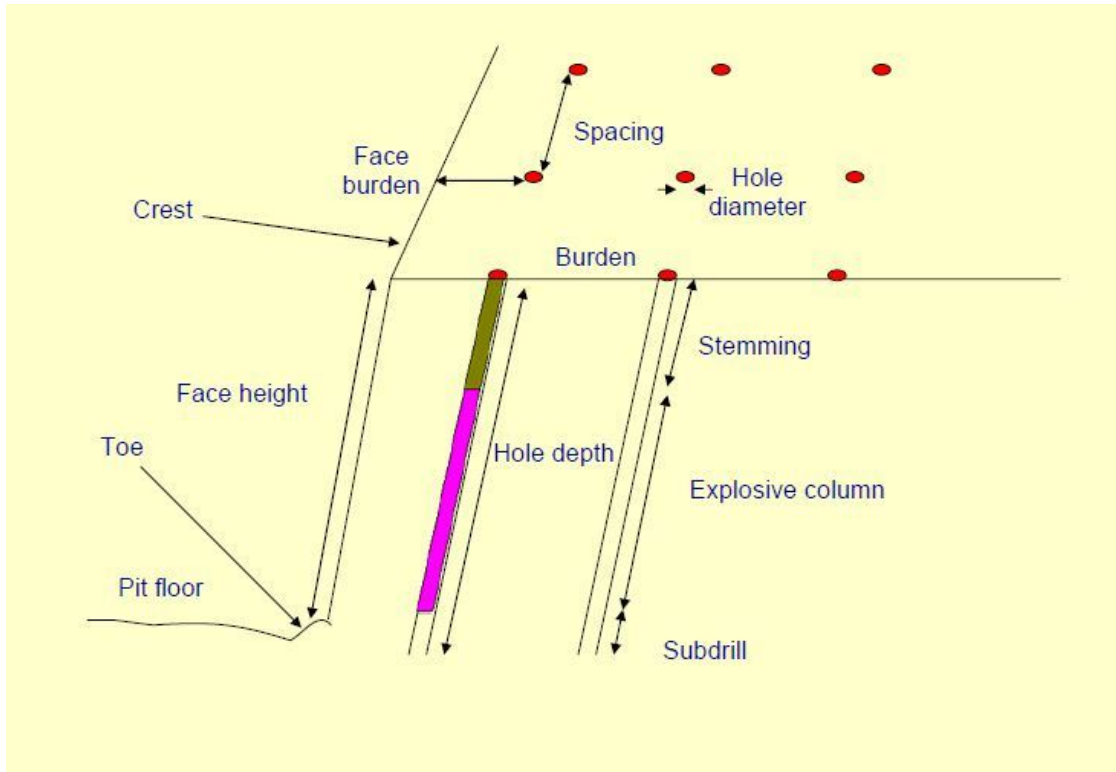


Figure 1: Bench blast geometry and terminology (Onlineminingexam, 2018).

The primary requisites for any blast design are that it ensures optimum results for existing operating conditions, possesses adequate flexibility and is relatively simple to employ. Several

factors affect the output of a blast. These factors can be generally classified into two main groups:

- Uncontrollable factors; and,
- Controllable factors

The blast design must aim at providing adequate fragmentation and ensuring that loading, haulage and subsequent processing is accomplished at the lowest possible cost (Muhammad, 2009).

## **2.4. Uncontrollable Factors**

Uncontrollable factors are those that the blaster has no control over. They are controlled by the properties and behavior of the in-situ formation to be blasted. According to Konya and Walter (1990), these factors include: geology, rock characteristics, regulations as well as the distance to the nearest structures. These constraints usually require that the blaster makes a modification to a standard design to fit the conditions of the site.

### **2.4.1. Rock Geotechnical Properties**

For optimum blasting performance, it is essential that the influence of rock mass properties on the blasting process be well understood. Rocks are usually characterized by several properties. The nature and properties of the rock mass vary sharply over short distances. It is therefore important that the influence of the rock mass parameters be well understood during the blast design process (Bhandari, 1997).

#### **2.4.1.1. Rock Strength**

Rock strength is measured as the force under which rocks fails or breaks. Rocks can fail in three ways: compression, tension and shear. Rock is generally strongest in compression, so blast designs should strive to place the rock in tension for breakage and in shear for creating

smooth surfaces, such as in presplitting (ISSE Blasters' Hand Book pp128). Table I, classifies rocks by compressive strength.

**Table I: Engineering classification of rock by compressive strength, Marinos & Hoek (2001).**

Grade	Classification	Field identification	Unconfined compressive strength (MPa)	Point Load Index (MPa)	Examples
R0	Extremely weak	Indented by thumbnail	< 1	-	Stiff fault gouge
R1	Very weak	Peeled with a pocket knife.	1 – 5	-	Highly weathered or altered rock
R2	Weak	Peeled with a pocket knife with difficulty	5 – 25	-	Chalk, claystone, potash, shale
R3	Medium strong	Cannot be peeled with a pocket knife	25 – 50	1 – 2	Concrete, phyllite, schist
R4	Strong	Requires more than one blow to fracture	50 – 100	2 – 4	Limestone, marble, sandstone
R5	Very strong	Requires many blows to fracture	100 – 250	4 – 10	Amphibolite, sandstone, basalt
R6	Extremely strong	Can only be chipped	>250	>10	Fresh basalt, granite

#### **2.4.1.2. Elasticity**

The elasticity is the ratio of the applied stress to its corresponding strain in elastic materials. Common terminologies used are Young's modulus of elasticity and coefficient of elasticity (ISEE Blasters Hand Book pp128).

The modulus of elasticity characterizes the rigidity of rock and its capacity to resist external influences. It is difficult for the explosive gases to compress and stretch the rock if Young's modulus of the rock is high. It is found that gas pressure should be less than 5% of Young's modulus for efficient blasting (Anon, 1980).

#### **2.4.1.3. Density**

Rock density is its mass per unit volume, where the ratio of its density to the density of water is called its specific gravity. Blast designers use rock density to design proper energy or powder factors. For blasters, accurate densities are important when converting rock volumes to weights for blast log properties (ISEE Blasters' Hand Book pp127).

In general, the ease or difficulty in breaking the rock is dictated by the density of the rock. It indicates the energy needed to deform and displace the rock and affects the energy propagation properties of the rock. However, porous rocks having lower density absorb energy and make fragmentation difficult (Bhandari, 1997).

#### **2.4.1.4. Porosity**

Rock porosity is a measure of the void space within a rock. A highly porous rock has a high percentage of voids or pore spaces. These voids or open spaces can increase the potential for a rock to take in and possibly hold water. Extreme porosity with vesicular basalt can effectively reduce explosive energy confinement (ISEE Blasters' Hand Book pp 128).

Porosity of rocks also affects the blasting performance. During blasting of highly porous rocks, greater dissipation of energy takes place and considerable crushing and production of fines occur. The work of fragmenting highly porous rock therefore, is performed almost entirely by the heave energy component of an explosive's total energy output. Porous rocks are susceptible to influence of pore water pressure which reduces the compressive and shear strength considerably (Obert & Duvall, 1967). When such rocks become saturated, blast effects are intensified (Ash, 1968).

#### **2.4.2. Rock Structure**

Rocks are generally heterogeneous and anisotropic. Variability of rock properties is important to blasting as it helps in predicting the spread of the fragmentation in the blasted material. The differences are usually due to the origin of formation and structural features such as bedding planes, fractures, faults, etc. The influence of these structural features on the response of the rock mass to applied loads cannot be ignored during blast design as the rock strength, deformation characteristics and strain wave propagation are dependent on their nature, location, properties and orientation. Many researchers who studied the influence of rock structures on blasting concluded that these structural features have a greater influence on blast results than the explosive properties and blast geometry (Bhandari, 1997).

#### **2.5. Controllable Factors**

These are factors over which the blast engineer has control and should be selected to overcome the challenges posed by the uncontrollable variables. Controllable parameters in blast design can be grouped into geometrical and explosive parameters.

### 2.5.1. Geometrical Parameters

The geometrical parameters include hole diameter, hole depth, sub drill depth, bench height, stemming height and material, burden and spacing.

#### 2.5.1.1. Hole Diameter

The hole diameter is selected to give the required fragmentation for loading, hauling and processing, and to meet the production requirements. The hole diameter plays an important role in the distribution of explosives in a given blast. Small diameter holes are good in highly jointed rocks. Large hole diameters give reliable explosive detonation, higher shock energy, lower drilling and blasting cost and higher productivities. The selection of the hole diameter depends on the bench height, machines available, degree of fragmentation required, type of explosive and rock properties (Muhammad, 2009). Equation 1, below shows the formula in calculating hole diameter.

$$HD \text{ (inches)} = \frac{BH}{5} \quad \text{Equation (1)}$$

where, HD is hole diameter in inches, BH is bench height in foot (Anon, 2010).

#### 2.5.1.2. Sub drill Depth

Sub-drilling is the term that defines the depth to which a blasthole will be drilled below the proposed grade or floor level. To ensure that the blast provides adequate fragmentation to the desired grade, it is necessary to drill below the desired grade. This sub-drilling is necessary because of the nature of rock breakage; when the explosive is detonated the rock at the bottom of the blasthole is the most difficult to break, since it is most confined. It is advisable to sub-drill to a depth of at least 0.3 to 0.5 times the burden below the desired elevation to increase the magnitude of the tensile stress at floor level. The sub-drilling will vary depending on the type of rock (Hemphill, 1981).

### 2.5.1.3. Bench Height

One of the primary factors that controls the design of a blast is the bench height. Usually, the bench height,  $BH$ , is relatively constant for most multi-level pits and its value is set to conform to the working specifications of loading equipment (Bhandari, 1997).

Bench heights vary within wide limits. In large open pits from which stone or minerals are mined, bench heights of 50 – 65 feet are common, although benches with heights up to 100 feet are occasionally encountered. In many places, bench heights are limited as safety precaution. The bench height can be determined with Equation 2, below (Anon, 2010). In general, faces with heights of about 30 – 60 feet have been considered the most economical and least hazardous to work in open pit metal mines. Where it is necessary to practice selective mining/quarrying, the face height may be dictated by the thickness of ore/rock of a certain quality (Bhandari, 1997).

$$BH = CD \times 5 \quad \text{Equation (2)}$$

where,  $BH$  is bench height in foot,  $CD$  is charge diameter in inches (Anon, 2010).

### 2.5.1.4. Stemming Height and Material

Stemming height is the length of the blasthole which is normally filled with inert material to confine the explosive gases. The primary function of stemming is to confine the gases produced by the explosive until they have adequate time to fracture and move the ground. The type and length of stemming have no significant effect on the characteristics of the explosion generated strain-waves and hence does not increase stress-wave effect. The amount of unloaded collar required for stemming is generally from one-half to two thirds of the burden dimension (Bhandari, 1997).

There is an optimum stemming length which further increments in stemming column serve no useful purpose. Ash (1968) recommended stemming lengths varying from  $1/2 - 2/3$  the

burden value, depending on strata conditions. Smaller stemming columns of less than 20 times the diameter of hole may result in more ground vibrations. The air blast levels created due to blasting are a function of the amount and efficiency of the stemming. If insufficient stemming is used, blowing out of stemming material may occur before gaseous energy is effectively utilized for fragmenting and displacing rock. Konya et al. (1981), in their studies found that the type and length of stemming controls the air blast. Their results indicated that stemming particle size of about one fourth of the blast hole diameter provides the best confinement. They suggested the stemming to burden ratio between 1 – 1.5. In the absence of blowing out of stemming air blast overpressure are known to drop by about 90% (Konya & Walter, 1990). Air blasts could be minimized by using coarse and angular stemming material. Hagan & Kennedy (1977), recommended a stemming column of at least 25 times that of blasthole diameter or about equal to burden, to minimize the air blast problem.

#### **2.5.1.5. Burden**

The burden  $B$ , is the distance from a charge axis to the nearest free face at the time the hole detonates. The free face is created by a row of holes that have been previously shot on an earlier delay. The burden is also defined as the distance from the first row of holes to the face of the excavation or between rows in the usual case where rows are fired in sequence. Too small burdens result in a throw over considerable distance, high air blast levels and excessively fine fragmentation. Too large burdens may also result in severe back break, over confinement of the explosives which can cause high ground vibrations and extremely coarse fragmentation. It can also result in toe formation. Of all the parameters of blast design, the burden has the least allowable error. The burden can be estimated using equation 3.

$$B = D_e \times \left( 2 \times \left[ \frac{d_e}{d_r} \right] + 1.5 \right) \quad \text{Equation (3)}$$

where,  $B$  is the burden in feet (ft),  $D_e$  is the diameter of fully coupled explosive column in inches (in),  $d_e$  is the density of the explosives (g/cc) and  $d_r$  (g/cc) is the density of the rock (Anon, 2010).

#### **2.5.1.6. Spacing**

Spacing is an important parameter in blast design. It is defined as the distance between any two adjacent charges in the same row and it controls mutual stress effect between charges. Spacing is calculated as a function of burden, hole depth, relative primer location between adjacent charges and depends upon initiation time interval. The spacing is usually from 1 to 1.8 times the burden (Mishra, 2009).

When the spacing is appreciably less than the burden, premature splitting between the blastholes and early loosening of the stemming material tend to occur. This causes a rapid release of the explosive gases at high pressure into the atmosphere and considerable back break. When the spacing to burden ratio is too high, adjacent charges cannot interact well to break the intact rock between them and will result in boulder formation (Bhandari, 1997). Spacing is calculated as a function of burden, hole depth, relative primer location between adjacent charges and also depends upon initiation time interval. The spacing is selected according to widely held concept that since the break angle made by the charge to the bench face is near  $90^\circ$  hence spacing larger than two times the burden are not possible (Gregory, 1973).

#### **2.5.2. Explosive Factors**

This includes the type of explosives and properties of explosives such as powder factor.

### 2.5.2.1. Powder Factor

Powder factor (sometimes also referred as charge factor) is the ratio between the total weights of explosive detonated in a blast divided by the amount of rock that is broken. It is usually expressed as Pounds per cubic foot (lb/ft<sup>3</sup>) (Bhandari, 1997).

As the powder factor in lb/ft<sup>3</sup> increases, the average fragment size decreases when the burden remains constant (Gustafsson, 1981).

In order to obtain good fragmentation and thereby ease in loading operation, the explosive consumption in excavation is somewhat greater than in quarrying. When firing is confined to a single row of blastholes in soft laminated strata, the charging ratios may be as low as 0.15 – 0.25 kg/m<sup>3</sup>. In harder sedimentary strata the charging ratios generally are around 0.45 kg/m<sup>3</sup> while they may be about 0.6 kg/m<sup>3</sup> in jointed igneous rock (Gustafsson, 1981). The powder factor can be determined by Equation 4 as presented by (Anon, 2017).

$$PF = \frac{W_e}{V} \quad \text{Equation (4)}$$

where, PF is powder factor (lb/yd<sup>3</sup>),  $W_e$  is total weight of explosive used in blast (lb) and  $V$  is volume of rock generated in blast (yd<sup>3</sup>).

### 2.5.2.2. Type and Properties of Explosives

The output of a blast is highly dependent on the type and properties of the explosives used. Explosive properties that affect blast output include density, velocity of detonation, detonation pressure, water resistant and explosive strength. The higher the density, energy, velocity of detonation and detonation pressure of an explosive, means the finer the fragmentation expected if all other design parameters are the same (Bhandari, 1997).

The density of an explosive affects its sensitivity. The lower the density, the higher the sensitivity of the explosive. Also, in wet blastholes, water resistant explosives must be used to

maintain their potency. Due to environmental constraints, explosives that produce lesser quantities of fumes and less dangerous fumes should be used especially in confined spaces.

## **2.6. Fragmentation Analysis**

Methods to quantify the size distribution of fragmented rock after blasting are grouped as direct and indirect methods. Sieving analysis of fragments is the only direct method. Although sieve analysis is the most accurate technique among others, it is not practical on a large scale due to being both expensive and time consuming. For this reason, indirect methods which are observational, empirical and digital methods have been developed.

Observational method depends on experts common sense is a widely used technique. An engineer assesses the fragmentation and other blasting results subjectively. This method is not a scientific method as it does not give any information about the size distribution (Jimeno et al, 1995).

The most popular method to quantify the fragmentation is the determination of the size distribution using imaging processing techniques. It is the second most accurate method after sieve analysis (Higgins et al, 1999) and (Kemeny et al, 1999). In this method, images can be acquired from muck piles, haul trucks, leach piles, draw points, waste dumps, stockpiles, conveyor belts, etc.

There are several software's commercially available to quantify the size distribution namely Split-Desktop<sup>®</sup>, WipFrag<sup>™</sup>, PowerSieve etc. This research used Split-Desktop<sup>®</sup> Software because it was in use at the mine due to its user friendliness.

### **2.6.1. Split-Desktop<sup>®</sup> Software**

Split-Desktop<sup>®</sup> is an image processing program for determining the size distribution of rock fragments at various stages of rock breaking in the mining and processing of mineral

resources. The desktop version of Split refers to the user-assisted version of the program that can be run by mine engineers or technicians at on-site locations. The desktop Split system consists of the Split software, computer, keyboard and monitor. There must be a mechanism (software and/or hardware) for downloading digital or video camera images onto the computer. For digital cameras the software that is supplied with the camera is required and for video camera images a frame grabber board is necessary. For higher resolution images and for ease of image selection, than is available by most frame grabbers, a digital camera is recommended. The first step is for the user to acquire images in the field and download these images onto the computer. The source of these images can be a muckpile, haul truck, leach pile, draw point, waste dump, stockpile conveyor belt, or any other situation where clear images of rock fragments can be obtained. The Split program first assists the user in properly scaling the images using the scale ball placed in the photograph. Split can then automatically delineate the fragments in each of the images and determine the size distribution of the rock fragments. Split allows the resulting size distributions to be plotted in various forms (linear-linear, log-liner, log-log and Rosin-Rammler). The size distribution results can also be stored in a tab-delineated file for access in separate spreadsheet and plotting programs (Kemeny et al, 1999).

The desktop version of the Split program has five major parts. The first part of the program concerns the scaling of images taken in the field. The second part of the program deals with the automatic delineation of the fragments in each of the images that are processed. The third part of the program allows the editing of the delineated fragments to ensure high quality results. The fourth part of the program involves the calculation of the size distribution based on information from the delineated fragments. Finally, the fifth part of the program concerns the

plotting or export of the size distribution results (Girdner et al, 1996). Each of the five parts of the program are described below.

#### **2.6.1.1. Image Acquisition and Scaling**

There are many ways that images can be acquired in the field and scaled. For instance, if images are taken along a moving conveyor belt, the scaling of the images is straightforward and can be as simple as measuring the width of the belt. When acquiring images of muckpiles, the angle of slope relative to the axis of the camera needs to be considered. If it is not perpendicular, the scale as represented in the image varies continuously from the bottom of the slope to the top of the slope. There are several ways to correct the scale in muckpiles (Kemeny et al, 1999) and (Girdner et al, 1996). The simplest way is to place two objects of known size in the image, one near the bottom of the slope and one near the top of the slope, as shown in Figure 2. To eliminate side-to-side distortion, all pictures should be taken perpendicular to the line of the toe of the slope.



**Figure 2: A large scale muckpile image.**

Three scales of image which are large scale (20×20 feet), medium scale (10×10 feet) and small scale (1.5×1.5 feet) are required when using Split. Equal numbers of images at each scale should be acquired. If one is not interested in the size distribution of the smallest scale of the material and is happy to accept Schumann or Rosin-Rammler curve in this range, taking the small-scale images may be omitted. Figure 2, Figure 3 and Figure 4 show that images acquired at large scale, medium scale and small scale respectively. While taking the images, lighting is important. Best lighting is provided in overcast days due to even lighting and fewer shadows (Girdner et al, 1996).



**Figure 3: A medium scale muckpile image.**



**Figure 4: A small scale muckpile image.**

### **2.6.1.2. Fragment Delineation**

Once the images have been acquired and scaled, the next step is for Split-Desktop<sup>®</sup> to delineate the individual rock fragments in each of the images. Lighting corrections and auto thresholding algorithms are used. After preprocessing and auto-thresholding, the Split-Desktop<sup>®</sup> program automatically delineates the fragments using a set of algorithms based on the following four steps; gradient filter, shadow convexity analysis, Split algorithm and Watershed algorithm (Girdner et al, 1996) and (Kemeny et al, 1999).

### **2.6.1.3. Editing of Delineated Image**

In most muckpile images and in many images from other sources such as haul trucks or leach piles, there are instances when the automatic delineation algorithms in Split will not delineate the fragments properly. This may be due to situations where the lighting is poor, there is an abundance of fines in the image, and the image quality is low or other reasons. In these cases, the delineated images needs to be edited using hand editing tools in the program. There are three common cases where minor editing is needed. First, if there are large patches of fines in the image, Split sometimes mistakes these patches as a single large fragment. Second, if there is excessive “noise” on a fragment (due to bedding, rock texture, etc.), the Split program may divide this fragment into a number of smaller fragments. Third, some of the delineated particles are neither rock fragments nor fines and should not be counted in the final size distribution, such as the scale balls or ruler in the muckpile images. However, the following limitations of image analysis have been identified. Delineation of particles might be limited due to disintegration and fusion of particles and the transformation of surface measurements of particles into volumes may not be representative of the particles being sampled (Bamford, 2016). Figure 5 shows a complete delineated muckpile image.

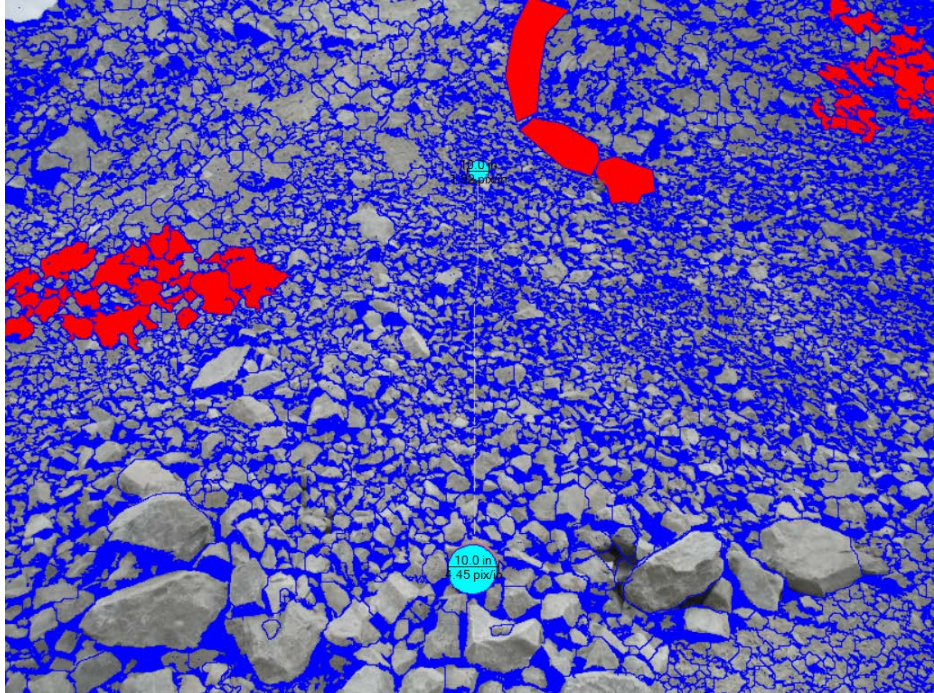


**Figure 5: Delineation of the muckpile image with masked scale balls (light blue) and fines fill (red).**

Split-Desktop<sup>®</sup> has built in editing capabilities to handle the situations described above. The Split program first makes a stack of images, where one file in the stack is the delineated image pasted over the original grayscale image and the other file in the stack is the original grayscale image. The user can quickly toggle between the original and delineated images to determine which parts of the image need editing. Three kinds of editing are most common; paint bucket filling of fines, erasing unwanted delineations, and identifying non-rock features such as scaling objects. In most cases a skilled user can edit the images in less than three minutes (Kemeny et al, 1999).

#### **2.6.1.4. Calculation of the Size Distribution**

Once the individual fragments in the images have been delineated, the next step is to use characteristics of the fragments to calculate the size distribution. These characteristics include the area and dimensions of each fragment and the area of the non-particle regions (Red areas). Screen size and volume of each fragment from these characteristics are determined.

The second step is to determine a realistic distribution for the fine material. Two options for the distribution within the fines are available in Split, a Schumann distribution and a Rosin-Rammler distribution. Each of these distributions has two unknown parameters and these parameters are determined from two known points in the size distribution, one point at the fine size and the other at 1.5 times the fine size.

### 2.6.1.5. Presentation of the Size Distribution Results

Once the size distribution has been calculated, it can be plotted in four ways; linear-linear plot, log-linear plot, log-log plot and Rosin-Rammler plot. Figure 6 is an example of a log-linear plot. Next to each plot, the size distribution data is also printed in one of four formats (ISO standard, British standard, US standard, no standard). The 20<sup>th</sup> percentile of the particle size distribution, P20, mean fragment of the particle size, P50, 80<sup>th</sup> percentile of the particle size distribution, P80 and top size are also shown. The size distribution and percent passing sizes are written to files stored on the hard disk in text format for further manipulation in separate database or plotting programs.

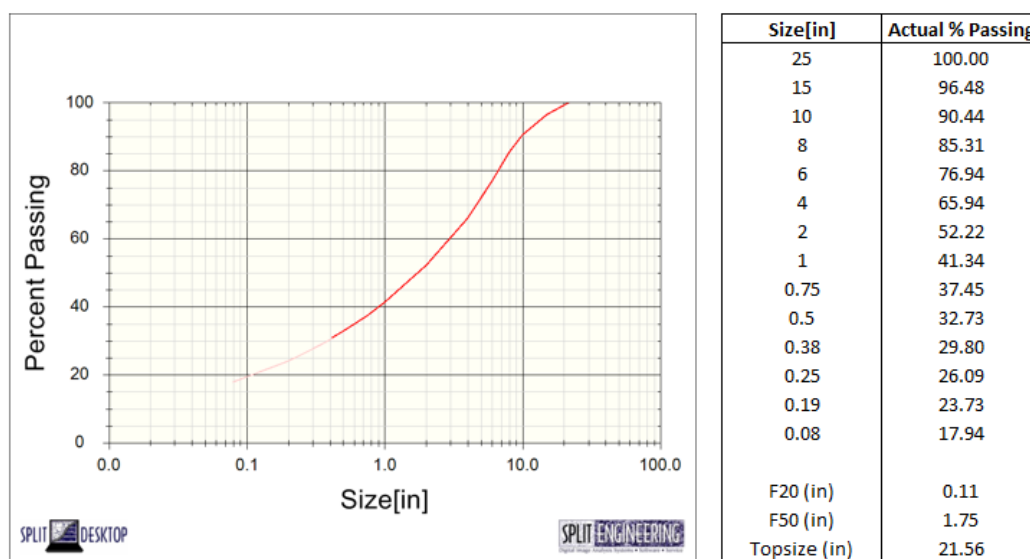


Figure 6: Log-Linear Size distribution plot result.

## 2.7. Fragmentation Modelling/Prediction

A number of different fragmentation models have been developed over the years. In most of the models the average fragment size,  $X_{50}$ , is calculated and some of the models describes the whole fragment size distribution. The input parameters to the models are rock properties, explosive properties and the geometric design of the blasts. The designs of the blasts are known and the explosive properties for the models can be found by simple tests, but the mechanical properties of the rock are more difficult to obtain, i.e. the strength of the rocks in heterogeneous rock and the joint properties in bench blasting where no free surfaces can be found. The difficulties obtaining the rock properties gives that the accuracy of the fragmentation models are relatively poor, but they provide an indication of the influence of changing the design of the blasts (Bergman, 2005).

The models for prediction of size distribution are generally classified into two categories; empirical and mechanistic models. The empirical models assume that finer fragmentation is a result of higher input energy from explosives i.e. through higher powder factors. The mechanistic models track the physics of detonation and energy transfer for specific blast designs. The mechanistic models are not popular in practice because they are very sophisticated and require more input data (Johnson, 2014).

Due to the sophisticated nature of the mechanistic models, empirical models are most common in practice. This thesis makes a comparison of the Kuz-Ram model and Modified Kuz-Ram model to see which model best predicts the size distribution of fragments observed at the mine.

### 2.7.1. Kuz-Ram Model

A variety of modelling approaches, ranging from purely empirical to rigorous numerical models have been used to predict fragmentation from blasting and the most popular is the Kuz-Ram model developed by Cunningham in 1983. Cunningham modified the Kuznetsov's empirical equation to estimate the mean fragment size ( $x$ ), and used the Rosin-Rammler distribution to describe the entire size distribution. The uniformity exponent of the Rosin-Rammler distribution is estimated as a function of the blast design parameters (Cunningham, 1987).

The Kuz-Ram model predicts fragmentation from blasting in terms of mass percentage passing a given mesh size with the following assumptions, i.e. finer fragmentation results from higher explosive energy, weak rocks and smaller blasthole diameters and more regular fragmentation sizing results from the uniform distribution of explosives in the rock mass, small burdens and greater spacing to burden ratios (Choudhary and Gupta, 2012). The Kuz-Ram model for the prediction of rock was first presented at the 1983 Lulea conference on fragmentation by blasting. Since then, the model has been evaluated, improved and likely surpassed in performance by more complex fragmentation models. However, it is a simple model that gives reasonable approximations of blasting fragmentation results and it is a three parameter fragment size distribution model, consisting of the Kuznetsov's equation, the Rosin-Rammler's equation and Cunningham's Uniformity index (Adebola et al, 2016). These three equations define three different parameters that constitute the prediction output model.

#### 2.7.1.1. Kuznetsov's Equation

Kuznetsov (1973), developed an equation for determining the mean fragment size, denoted as ( $X_{50}$ ) as shown in Equation 5.

$$X_{50} = AK^{-0.8} \times Q^{\frac{1}{6}} \left( \frac{115}{REE} \right)^{\frac{19}{20}} \quad \text{Equation (5)}$$

where, A is the rock factor, Q is the mass of explosive been used in kg, K is the powder factor (specific charge) in kg/m<sup>3</sup> and REE is the relative effective energy of the explosive, this is derived by dividing the absolute weight strength of the strength of the explosive in use by the absolute weight strength of ANFO and multiply by 100%. The mean fragment size is the first estimated to give an overview of what outcome will be generated by the blast design parameters for effective predictive process.

#### 2.7.1.2. Rosin-Rammler's Equation

The Rosin-Rammler's equation for percentage passing is determine in Equation 6. This is also important in characterizing muckpile size distribution (Faramarzi, et al., 2013)

$$R_x = \exp \left[ -0.693 \left( \frac{X}{X_m} \right)^n \right] \quad \text{Equation (6)}$$

where,  $R_x$  is the mass fraction retained on screen opening X, n is the uniformity index usually between 0.7 and 2 based on the blast geometry; and  $X_m$  is the mean particle size.

The percentage passing (% passing) represents the percentage of material that will pass through a screen of a particular mesh size (X) is found by Equation 7.

$$\% \text{ passing} = 1 - R_x = 1 - \exp \left[ -0.693 \left( \frac{X}{X_m} \right)^n \right] \quad \text{Equation (7)}$$

#### 2.7.1.3. Cunningham's Uniformity index

Cunningham established the applicability of uniformity coefficient through several investigations by considering the effects of blast geometry, hole diameter, burden, spacing, hole length and drilling accuracy. This can estimated using Equation 8 as shown below.

$$n = \left[ 2.2 - 14 \left( \frac{B}{D} \right) \right] \left[ 0.5 \left( 1 + \frac{S}{B} \right) \right]^{0.5} \left[ 1 - \frac{W}{B} \right] \left[ \text{abs} \left( \frac{BCL - CCL}{L} \right) + 0.1 \right]^{0.1} \left[ \frac{L}{H} \right] \quad \text{Equation (8)}$$

Where, B is the burden (m), S is the spacing (m), D is the hole diameter (mm), W is the standard deviation of drilling accuracy (m), BCL is the bottom charge length (m), CCL is the column charge length (m), L is the total length of drilled hole (m) and H is the bench height (m).

Cunningham proposed the model in its most basic form, wherein the parameters required for the fragmentation prediction were basically controllable elements of the blast design.

The rock factor, A is used to modify the average fragmentation based on the rock type and blast direction. The rock factor is calculated by Equation 9 originally developed by Lilly in 1986.

$$A = 0.06(RMD + RDI + HF) \quad \text{Equation (9)}$$

Where, RMD is the rock mass description i.e. 10 (powdery/friable), JF (if vertical joints) and 50 (if massive), RDI is the rock density influence and HF is the hardness factor.

Figure 7 shows the description of the rock properties and the values assigned to each component of the rock factor equation as described by Lilly, 1986.

	Parameter	Rating
1	Rock Mass Description (RMD)	
	Powdery/Friable	10
	Blocky	20
2	Joint Plane Spacing (JPS)	
	Close (<0.1 m)	10
	Intermediate (0.1 to 1 m)	20
3	Joint Plane Orientation (JPO)	
	Horizontal	10
	Dip out of face	20
	Strike normal to face	30
4	Dip into face	40
	Specific Gravity Influence (SGI) = 25*SG-50, where SG is the density in (t/m <sup>3</sup> )	
5	Hardness, Moh's scale, (H),	1 to 10

Figure 7: Rock Parameters Description and Ratings (Source: Lilly 1986).

The mean fragment size is mainly influenced by explosive parameters. Improved fragmentation can therefore be achieved by using an explosive with higher RWS or density which has an impact on the powder factor or specific charge. If the powder factor is increased by reducing the blast pattern i.e. while maintaining the hole diameter and spacing to burden ratio, the uniformity index (n) will increase and hence fragmentation will improve i.e. become finer (Vasileois, 2008).

The uniformity index, n, determines the shape of the fragmentation curve. High values on n gives uniform sizing i.e. small amount of fines and oversized material, normally n ranges from 0.8-2.2, (Cunningham, 1983). The effects of the blasting parameters on n are shown in Table II.

**Table II: Effect of blasting parameters on Uniformity Index (n), Cunningham (1983).**

<b>Parameter</b>	<b>n increases as parameter</b>
Burden/Hole Diameter	Decreases
Drilling accuracy	Increases
Charge Length/Bench Height	Increases
Spacing/Burden	Increases
Staggered Pattern	Increases by 10%

### **2.7.2. Modified Kuz-Ram Model**

The Modified Kuz-Ram model is similar to the original Kuz-Ram model but the Kuznetsov equation is modified by an additional factor of 0.073 included in the formula for the prediction of the mean fragment size (Gheibie et al., 2009). The reason is joint aperture is considered as an effective parameter. The uniformity index of the Kuz-Ram model is also replaced by a modified uniformity index which is based on the original uniformity index equation proposed by Cunningham and a blastability index (BI). This model is a two-parameter

fragmentation size distribution model that can easily be determined on the field. Its defects lie in the fact that it does not consider the effect of timing on fragmentation and has no upper limit for sizes. The Rossin-Rammler equation (Eqn. 6) and Cunningham's uniformity index equation (Eqn. 8) are maintained as in the original Kuz-Ram model. Equation 10 and Equation 12 below shows how the mean fragment size and blastability values are obtained (Gheibie et al., 2009).

$$X_m = 0.073BI \left(\frac{V_o}{Q_e}\right)^{0.8} \times Q_e^{\frac{1}{6}} \left(\frac{S_{ANFO}}{115}\right)^{\frac{-19}{30}} \quad \text{Equation (10)}$$

$$n' = 1.88 \times n \times BI^{-0.12} \quad \text{Equation (11)}$$

$$BI = 0.5(RMD + JPS + JPA + RDI + HF) \quad \text{Equation (12)}$$

where,  $X_m$  is the mean fragment size, cm; BI is the blastability index,  $V_o$  is the volume of rock broken by one blasthole,  $m^3$ ,  $Q_e$  is the mass of explosive in each hole, kg;  $S_{ANFO}$  is the relative weight strength of the explosive to ANFO,  $n$  is the uniformity index,  $n'$  is the modified uniformity index and RMD, JPS, JPA, RDI and HF have the same meanings as defined in Figure 7, above.

The volume of the rock broken by one blasthole  $V_o$  ( $m^3$ ) can be found by Equation 13.

$$V_o = B \times S \times H \quad \text{Equation (13)}$$

## 2.8. Statistical Analysis

Statistical comparison of the model estimates or predictions with the actual/observations is the most basic means of assessing the models' performance (Willmott and Matsuura, 2005). Several statistical methods exist for assessing the performance of a model. However, the Root Mean Square Error and Correlation and Regression Analysis method was used for this research.

### 2.8.1. Root Mean Square Error Method

One method of statistically assessing the performance of a model is the Root Mean Square Error (RMSE) method. The lower the RMSE, the better the model performance (Monjezi and Rezaei, 2011). The prediction errors of each model are determined using Equation 14.

$$e_i = P_i - O_i \quad \text{Equation (14)}$$

where,  $P_i$  is the model predictions and  $O_i$  is the actual observations. After the model errors are determined, the average model-estimation error are obtained using Equation 15.

$$e_\gamma = \left[ \frac{\sum_{i=1}^n W_i |e_i|^\gamma}{\sum_{i=1}^n W_i} \right]^{\frac{1}{\gamma}}, \gamma \geq 1 \quad \text{Equation (15)}$$

where,  $e_\gamma$  is the average model estimator and  $w_i$  is a scaling factor assigned each error estimate according to the influence on the total error.

When using the root mean square error technique, each error is assigned a weight of 1 with the assumption that each one has the same effect on the total error. Therefore,  $\gamma = 2$  and is established as shown in Equation 16 below.

$$RMSE = \left[ \frac{\sum_{i=1}^n |e_i|^2}{n} \right]^{\frac{1}{2}} \quad \text{Equation (16)}$$

### **2.8.2. Regression and Correlation**

Another method of assessing a model's performance is the use of the correlation coefficient  $R$ , which describes the strength of the linear relationship between the predicted and corresponding actual results. The correlation coefficient interprets the  $R$  values as;  $0 < R < 30\%$  implies weak correlation,  $30\% < R < 70\%$  implies moderate correlation and  $R > 70\%$  implies strong correlation (Barnston, 1992).

### 3. Data Collection and Analysis

#### 3.1. Introduction

This chapter describes the data used for the research work and the methods used in analyzing the data obtained. Data collection procedures used for the research are also described in this chapter.

#### 3.2. Data Collection

Data for the research obtained from the Western US open pit copper mine was acquired through field measurements, files and documents at the mine. The data included the geometric blast design, explosive data and rock parameter data in the pit. Eight blasts from the mine were considered.

##### 3.2.1. Geometric Blast Design Data

Geometric data set were obtained from the blast plans and reports of the mine. The blast design parameters for the Eight Blasts are presented in Table III. The square drilling pattern was used in all blasts.

**Table III: Geometric Blast Parameters at Continental Pit**

<b>Parameter</b>	<b>Blast #3053</b>	<b>Blast #3054</b>	<b>Blast #3056</b>	<b>Blast #3060</b>	<b>Blast #3062</b>	<b>Blast #3063</b>	<b>Blast #3065</b>	<b>Blast #3067</b>
Burden (ft)	25	30	25	23	23	23	23	23
Spacing (ft)	25	30	25	23	23	23	23	23
Bench height (ft)	40	40	40	40	40	40	40	40
Hole diameter (in)	9.87	9.87	9.87	9.87	9.87	9.87	9.87	9.87
Hole depth (ft)	40	40	40	47	44	42	42	43
Stemming (ft)	15	15	15	16.1	17.91	22.44	21.93	20.56

### 3.2.2. Explosives Data

Buckley Powder Company supplies the explosives for blasting at the copper mine and the explosive data. The bulk explosive used at the mine is called Differential Energy™, otherwise known as Delta E, which is an unsensitized bulk emulsion specifically formulated to be sensitized when loading at the blasthole using a chemical gassing technology. The density is 1.2 pounds per cubic foot and velocity of detonation is 17000 foot per second to 22000 foot per second. The bulk strength of this explosive is 815. The explosive data for the eight blasts are shown on Table IV.

**Table IV: Explosive Parameters of Blasts at Continental Pit**

<b>Parameter</b>	<b>Blast #3053</b>	<b>Blast #3054</b>	<b>Blast #3056</b>	<b>Blast #3060</b>	<b>Blast #3062</b>	<b>Blast #3063</b>	<b>Blast #3065</b>	<b>Blast #3067</b>
Total Charge (lbs)	533	533.01	533	1162.13	996.07	785.41	798.17	804
Tons blasted (tons)	160,217	153,703	107,258	150,871	98,958	55,157	102,203	123,292
Powder Factor	0.28	0.19	0.30	0.72	0.61	0.48	0.49	0.50
Density (lbs/ft)	35.5	35.5	38.2	39.4	39.4	39.4	39.4	39.4
Charge length (ft)	15	15	15	15	15	15	15	15

### 3.2.3. Rock Parameters

The rock data at the copper mine was obtained from the Geology Department. Data obtained included the Uniaxial Compressive strength, rock density, joint spacing and young's modulus to determine the Rock mass description (RMD), Joint plane spacing (JPS), Joint plane

angle (JPA), Rock density influence (RDI) and the Hardness Factor (HF) to build the predictive models. Table V summarizes the rock parameters of Continental pit.

**Table V: Summary of Rock Parameters at Continental Pit**

<b>Parameter</b>	<b>Value</b>
Uniaxial Compressive Strength (MPa)	150
Joint Spacing (m)	1.5
Rock Density (kg/m <sup>3</sup> )	2700
Young's Modulus (Gpa)	50
Rock Type	Granite
Rock Description	Strong and blocky with slight weathering

#### **3.2.4. Muckpile Image Sampling**

Pictures of the blasted muckpiles were sampled for fragmentation analysis using Split-Desktop<sup>®</sup> software. The pictures were obtained using a digital camera with a minimum of ten pictures for each blast. Scaling objects were used and were set apart in each of the images 20 foot, 10 foot and 1.5 foot respectively. These scaling objects were used in each image as reference sized objects which Split-Desktop<sup>®</sup> uses to estimate the size of fragments.

### **3.3. Data Analysis**

#### **3.3.1. Fragmentation Analysis**

Split-Desktop<sup>®</sup> fragmentation analysis software was used to analyze the images to quantitatively assess the fragmentation of the blasts at the mine. Ten images were analyzed for each blast and the individual image results were combined by the software to represent the fragmentation of the blast. The images were delineated automatically after the scales were set but the results of the auto delineation were not representative of the image such that bigger fragments were split into several small delineated fragments while the smaller fragments were merged together and delineated as one object in the image. To ensure that the fragments were delineated properly, the images were edited manually by drawing borders around each rock fragment to completely delineate it and help the software to effectively estimate and measure the size of rock particles present in the images. A fine factor of 50% were used for the images because the software cannot delineate finer particles (less than 0.75 inches) hence using a fine factor the finer particle sizes present can be estimated. Voids between fragments were masked while areas of fine fragments whose edges were not clear enough to be delineated were masked as fines. The scaling objects were also masked so that they are not considered as rock fragments. Figure 11 shows a well delineated image with masked scale balls (light blue) and fines fill (red) in Split-Desktop<sup>®</sup>.

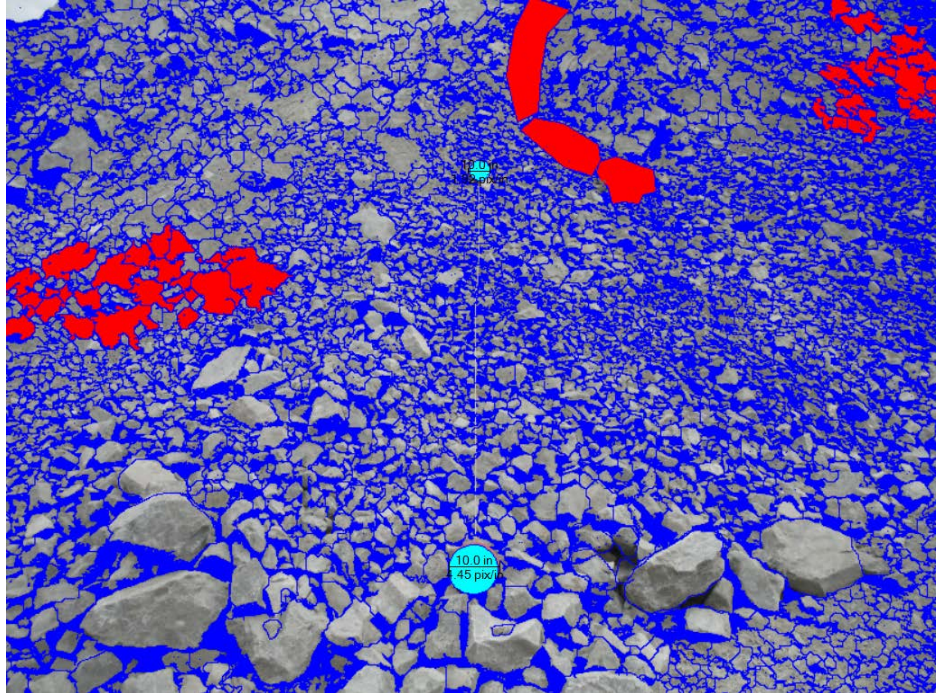


**Figure 8: Delineated muckpile image**

After the delineations were completed, the results were displayed in both graphical and tabular forms.

### **3.3.2. Fragmentation Prediction**

After data gathering, the geometric, explosive and rock parameters were used for the prediction of the fragmentation output for each of the blasts under study. The prediction was done using the Kuz-Ram and Modified Kuz-Ram models, chosen due to the following reasons:

- They are the most commonly used models in mining applications.
- The Modified Kuz-Ram model was introduced to remove some of the weaknesses of the Kuz-ram model.
- The data required as input for these models are relatively easy to gather.

A model (Figure 12) was developed in MS Excel 2016 for the prediction of the fragmentation size distribution.

Predictive Models developed using MS Excel 2016

Geometric Parameters	Value	Unit (Imperial)	Value	Unit (Metric)
Hole Depth	40	ft	12.19	m
Hole Diameter	9.87	in.	251	mm
Burden	25	ft	7.62	m
Spacing	25	ft	7.62	m
Bench Height	40	ft	12.19	m
Drill Deviation	0.32	ft	0.10	m
Drill Pattern (Square)	1		1	

Size (in)	Kuz-Ram %Passing	Modified Kuz-Ram %Passing
0	0.00%	0.00%
0.08	8.01%	7.33%
0.19	13.66%	13.13%
0.25	16.11%	15.73%
0.38	20.61%	20.59%
0.5	24.13%	24.44%
0.75	30.21%	31.20%
1	35.21%	36.80%
2	49.45%	52.83%
4	65.78%	70.78%
6	75.27%	80.64%
8	81.47%	86.66%
10	85.77%	90.57%
15	92.12%	95.72%
25	97.12%	98.92%

Explosive Parameters	Value	Unit (Imperial)	Value	Unit (Metric)
RWS of Explosive	815		815	
Charge Length	15	ft	4.57	m
Powder Factor	0.28		0.28	kg/m <sup>3</sup>
Stemming height	15	ft	4.57	m
Quantity of explosive per hole	533	lbs	242	kg
Explosive used per blast	90077	lbs	40858.2	kg

Rock Parameters	Value	Unit (Imperial)	Value	Unit (Metric)
Joint Spacing	5	ft	1.5	m
Undersize	0.75	in.	0.02	m
Optimal size	2.05	in.	0.05	m
Oversize	6	in.	0.15	m
Rock Factor	12.8			
Young's modulus	50	GPa	60	GPa
UCS	150	MPa	150	MPa
Rock mass description (RMD)	50			
Joint Plane Spacing (JPS)	50			
Joint Plane Angle (JPA)	40			
Rock Density influence (RDI)	17.5			
Hardness Factor (HF)	30			
Rock Description	2			
Rock Density of Granite			2700	kg/m <sup>3</sup>
Dip of Joints	3			

Kuz-Ram Model Parameters	Value
Mean fragment size X(50)	2.05
Uniformity Index (n)	0.652575
Characteristic size	0.035935

Modified Kuz-Ram Model Parameters	Value
Blastability Index	93.75
Mean fragment size X(50)	1.78
Modified Uniformity Index	0.711462



Figure 9: Kuz-Ram and Modified Kuz-Ram models in MS Excel 2016

### 3.3.3. Comparison of Model Performance

Using the results of the fragmentation analysis from Split-Desktop<sup>®</sup> as the baseline, the fragmentation prediction and image analysis were compared to determine the accuracy of the predictions made by each models. The statistical method used for this study was the Root Mean Square Error (RMSE) method and the correlation and regression method because they are frequently used to measure the difference between values predicted by a model and the values actually observed.

The root mean square of all the models were found relative to the actual fragmentation results obtained from Split and the model with the least RMSE value was taken as the best predictor. With the correlation and regression analysis, the model with the highest correlation coefficient, R and coefficient of determination,  $R^2$  values was considered as the best predictor models. The R values also establish the strength of the relationship between the model predictions and the actual fragmentation size distribution. The higher the R value, the better the relationship that exists between the predictions and the actual fragmentation results obtained from Split. Both methods were done using Microsoft Excel 2016.

## **4. Results and Discussions**

### **4.1. Introduction**

This section presents the results of the fragmentation analysis, prediction done through the use of the Root Mean Square Error analyses for all the blasts. A discussion of the results is also presented in this section.

### **4.2. Fragmentation Analysis**

The results and discussions for the fragmentation measurement obtained through image analysis in Split-Desktop<sup>®</sup> are presented in this section.

The fragmentation size distribution curves for each of the blasts considered at the Continental pit are presented in Figures 10 to 17. A summary of the fragmentation analysis results for the blasts at the Continental pit is shown in Table VI.

#### **4.2.1. Blast #3053**

From Figure 10, about 37.45% of the resultant fragments were fines (0.75 inches). The actual mean fragmentation (F50, 50% passing) of the blast was 1.75 inches while the top size (99.95% passing) was 21.56 inches below the crusher gape of 30 inches. This implies that the fragmentation is good as the top size has an insignificant percentage of (< 0.05%) boulders or no boulders were produced from this blast.



Figure 10: Fragmentation Size Distribution for Blast #3053

#### 4.2.2. Blast #3054

From Figure 11, the actual amount of fines (0.75 inches) produced was 34.51%, the measured mean fragmentation (F50 i.e. 50% passing) of the blast was 2.07 in while the top size (99.95% passing) was 22.98 in.

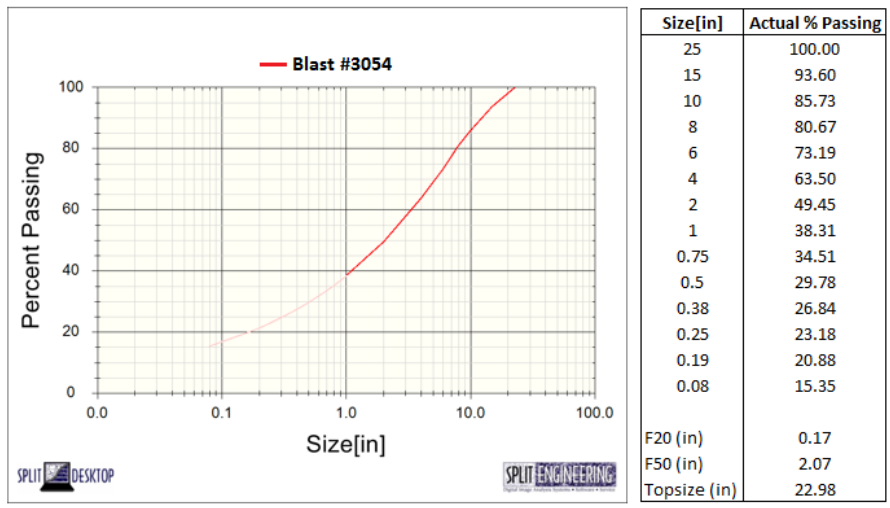


Figure 11: Fragmentation Size Distribution for Blast #3054

### 4.2.3. Blast #3056

The actual amount of fines (0.75 inches) produced from Blast #3056 as shown in Figure 12 was 28.67%, the top size (99.95% passing) was 27.20 inches meaning no boulders were produced. The measured mean fragmentation (F50 i.e. 50% passing) of the blast was 3.02 inches as shown in Figure 12.

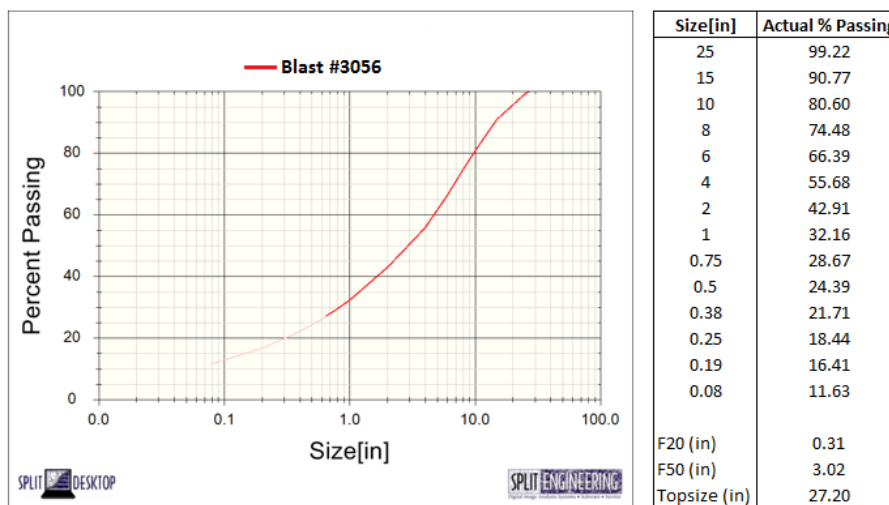


Figure 12: Fragmentation Size Distribution for Blast #3056

### 4.2.4. Blast #3060

As shown in Figure 13, 30.01% of the material blasted were fines since they had sizes less than 0.75 inches, the actual mean fragmentation (F50 i.e. 50% passing) was 2.23 inches while the top size (99.95% passing) was 19.36 inches below the crusher gape of 30 inches. This implies that about (< 0.05%) boulders or no boulders were produced for this blast.

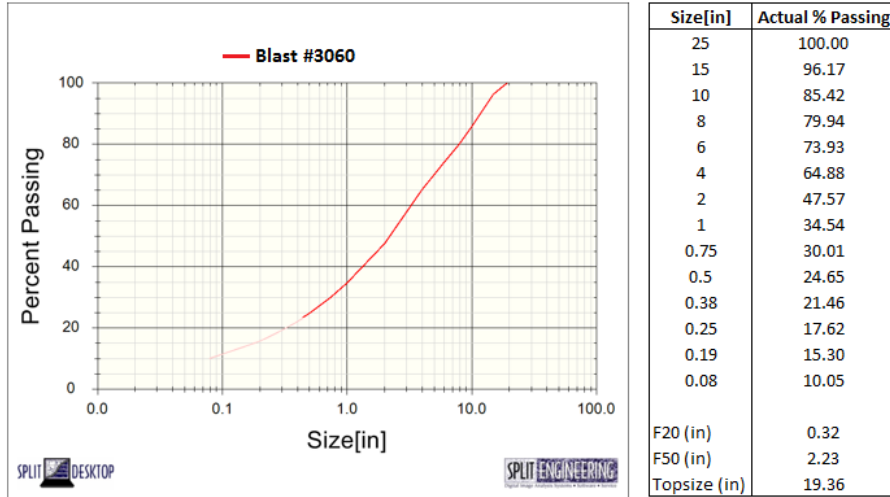


Figure 13: Fragmentation Size Distribution for Blast #3060

**4.2.5. Blast #3062**

The actual amount of fines (0.75 inches) produced from Blast #3062 as shown in Figure 14 was 26.33%, the top size (99.95% passing) was 12.55 inches meaning no boulders were produced. The measured mean fragmentation (F50 i.e. 50% passing) of the blast was 2.07 inches as shown in Figure 14.

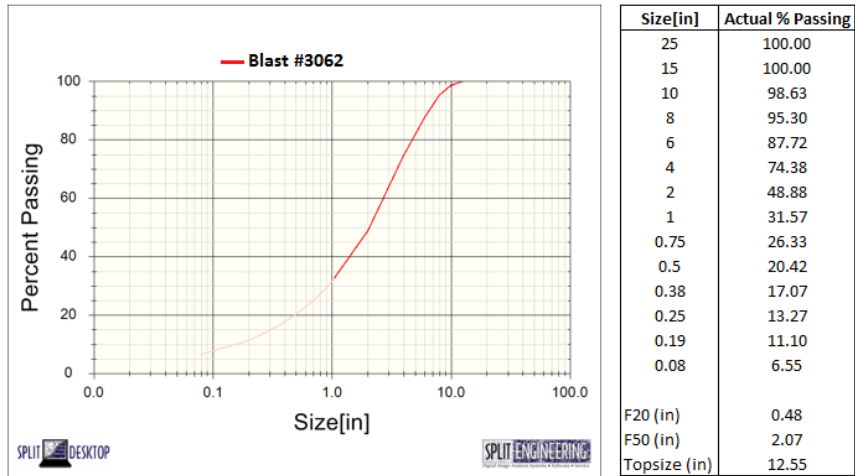


Figure 14: Fragmentation Size Distribution for Blast #3062

#### 4.2.6. Blast #3063

As shown in Figure 15, 25.95% of the material blasted were fines since they had sizes less than 0.75 inches. The actual mean fragmentation (F50 i.e. 50% passing) was 2.89 inches while the top size (99.95% passing) was 24.97 inches below the crusher gape of 30 inches. This implies that about (< 0.05%) boulders or no boulders were produced for this blast.

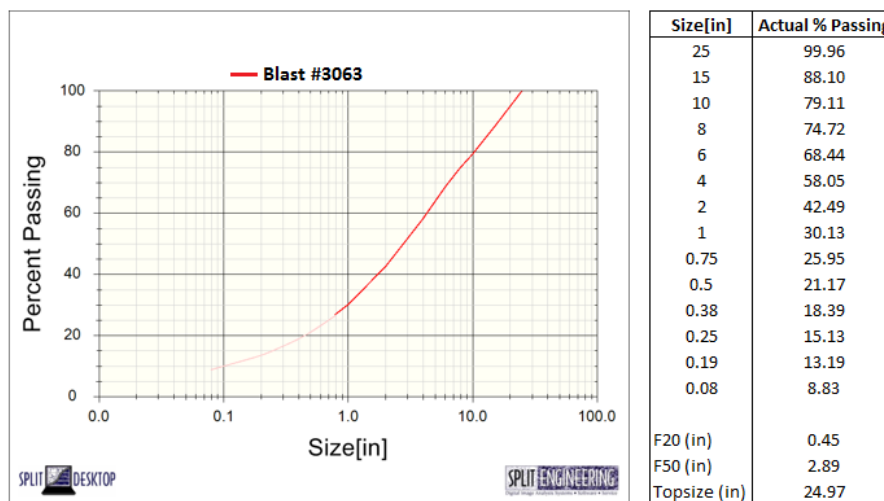


Figure 15: Fragmentation Size Distribution for Blast #3063

#### 4.2.7. Blast #3065

The actual amount of fines (0.75 inches) produced from Blast #3065 as shown in Figure 16 was 13.22%, the top size (99.95% passing) was 27.42 inches meaning no boulders were produced. The measured mean fragmentation (F50 i.e. 50% passing) of the blast was 4.34 inches as shown in Figure 16.

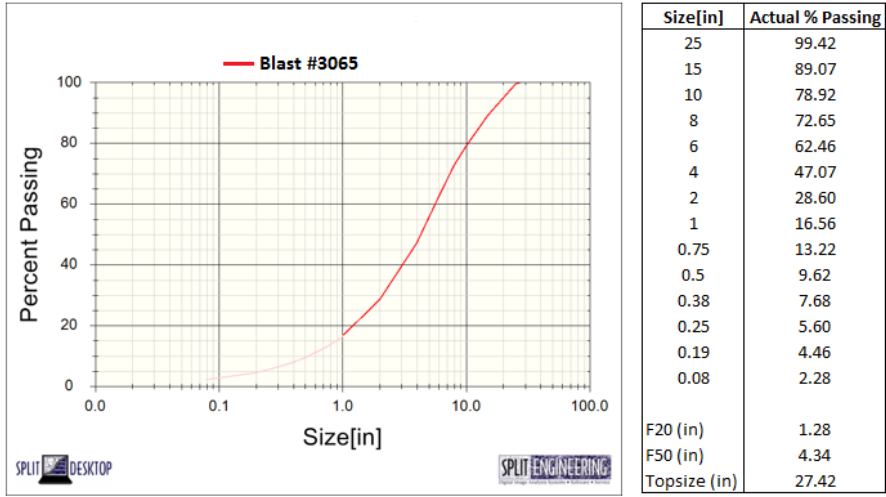


Figure 16: Fragmentation Size Distribution for Blast #3065

**4.2.8. Blast #3067**

From Figure 17, about 24.84% of the resultant fragments were fines (0.75 inches). The actual mean fragmentation (F50, 50% passing) of the blast was 3.36 inches while the top size (99.95% passing) was 31.47 inches almost the same as the crusher gape of 30 inches. This implies that the fragmentation is good as the top size has an insignificant percentage of 5% of the blasted material were considered as boulders or no boulders from the blast.

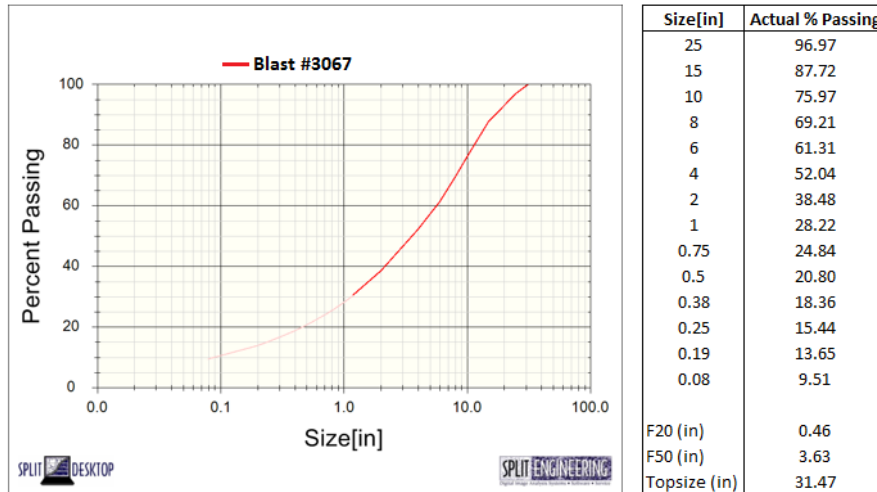


Figure 17: Fragmentation Size Distribution for Blast #3067

Table VI: Summary of Fragmentation Analysis Results for Blasts at Continental Pit

Size Fractions	Size (inches)							
	Blast #3053	Blast #3054	Blast #3056	Blast #3060	Blast #3062	Blast #3063	Blast #3065	Blast #3067
P10	0.01	0.02	0.05	0.08	0.16	0.1	0.53	0.09
P20	0.11	0.17	0.31	0.32	0.48	0.45	1.28	0.46
P30	0.38	0.51	0.84	0.75	0.92	0.99	2.13	1.15
P40	0.91	1.13	1.69	1.35	1.45	1.76	3.14	2.19
P50	1.75	2.07	3.02	2.23	2.07	2.89	4.34	3.63
P60	3.06	3.4	4.76	3.29	2.74	4.31	5.63	5.69
P70	4.69	5.3	6.81	4.98	3.55	6.41	7.38	8.22
P80	6.65	7.79	9.78	8.02	4.71	10.47	10.45	11.39
P90	9.8	12.37	14.5	11.86	6.5	16.08	15.67	16.46
Top size (99.95%)	21.56	22.98	27.2	19.36	12.55	24.97	27.42	31.47

### 4.3. Fragmentation Prediction

This section presents the results and discussions for the fragmentation prediction by the two models (Kuz-Ram and Modified Kuz-Ram) considered in this research.

The results of the fragmentation prediction for all the blasts at the Continental pit by Kuz-Ram and Modified Kuz-Ram against their Split-Desktop<sup>®</sup> fragmentation size distribution results are shown in Figure 18 to 24. The predictive results in tabular form are presented in Appendix A. Summaries of the fragmentation predictions for the Continental pit are presented in Tables VII to XIV while the summary of predicted and actual mean fragments sizes for the blasts are shown in Table XV.

#### 4.3.1. Blast #3053

Fragments from blasting with size less than 0.75 inches are considered as fines. The fines (< 0.75 inches) predicted by the Kuz-Ram and Modified Kuz-Ram models are 30.21% and 31.20% respectively as shown in Table VII. From the actual fragmentation measurement results obtained from Split-Desktop<sup>®</sup>, the fines (< 0.75 inches) produced from this blast were 37.45%. This implies that both the models under predicted the amount of fines produced. The percentage of under predictions by the Kuz-Ram and Modified Kuz-Ram models are 19.33% and 16.69% respectively.

The material which is within the desired range (0.75 inches and 25 inches) was predicted as 66.91% by Kuz-Ram and 67.72% for Modified Kuz-Ram as presented in Table VII.

Fragments with sizes above 25 inches are considered as Oversize. The oversize (> 25 inches) predictions were 2.88% and 1.08% by Kuz-Ram and Modified Kuz-Ram models respectively. The top size (99.95%) of this blast was 21.56 inches which is far below the 25

inches oversize criteria and hence an insignificant amount of oversize material was produced from the blast. This indicates over prediction of the oversize material by the fragmentation models with a difference of (< 3%).

The predicted mean fragment sizes for Blast #3053 as shown in Table XV are 2.05 inches and 1.78 inches for the Kuz-Ram and Modified Kuz-Ram models respectively. P50 for Blast #3053 which represents the actual mean fragmentation is 1.75 inches. The prediction errors were 17.14% and 1.71% for the Kuz-Ram and Modified Kuz-Ram models. Hence, the Kuz-Ram model over predicted the mean fragment of the blast while the Modified Kuz-Ram model closely predicted to the actual mean fragmentation with a difference of 2%.

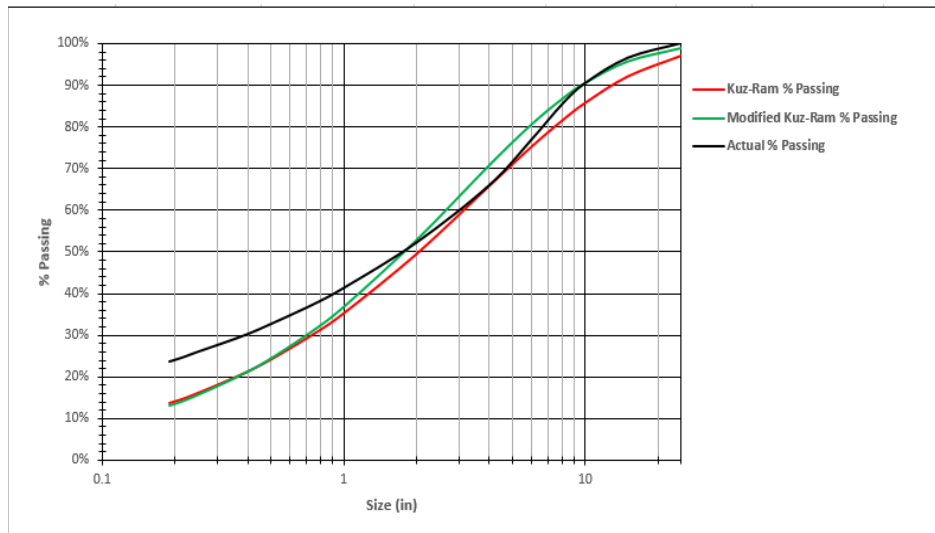


**Figure 18: Actual Size Distribution against Predictive Models for Blast #3053**

**Table VII: Fragmentation Prediction Summary for Blast #3050**

Fragment Size	Percent Passing (%)		
	Kuz-Ram	Modified Kuz-Ram	Actual Blast from Split (#3053)
Fines (< 0.75 inches)	30.21	31.20	37.45
Average (0.75 inches and 25 inches)	66.91	67.72	62.55
Oversize (>25 inches)	2.88	1.08	0

#### **4.3.2. Blast #3054**

The Kuz-Ram and Modified Kuz-Ram models predicted 36.27% and 37.85% of fines respectively to be produced from this blast. The actual amount of fines produced, however, was approximately 34.51%. The predictions were higher than the actual amount of fines produced. The percentages by which the prediction models exceeded the actual amount of fines are 5.09% for Kuz Ram and 9.68% for Modified Kuz-Ram respectively.

The oversize ( $> 25$  inches) predictions were 1.9% and 0.62% by Kuz-Ram and Modified Kuz-Ram models respectively. The top size (99.95%) of this blast was 22.98 inches which is below the 25 inches oversize criteria and an insignificant amount of oversize material was produced from the blast. This indicates over prediction of the oversize material by the fragmentation models with a difference of ( $< 2\%$ ).

The mean fragment sizes predicted by the Kuz-Ram and Modified Kuz-ram models are 1.50 inches and 1.31 inches respectively. The P50 which represents the actual mean fragmentation of the blast was 2.07 inches. There is therefore under prediction of the mean fragment sizes produced. The percentage under predictions are 27.54% and 36.71% for Kuz-Ram and Modified Kuz-Ram models respectively.

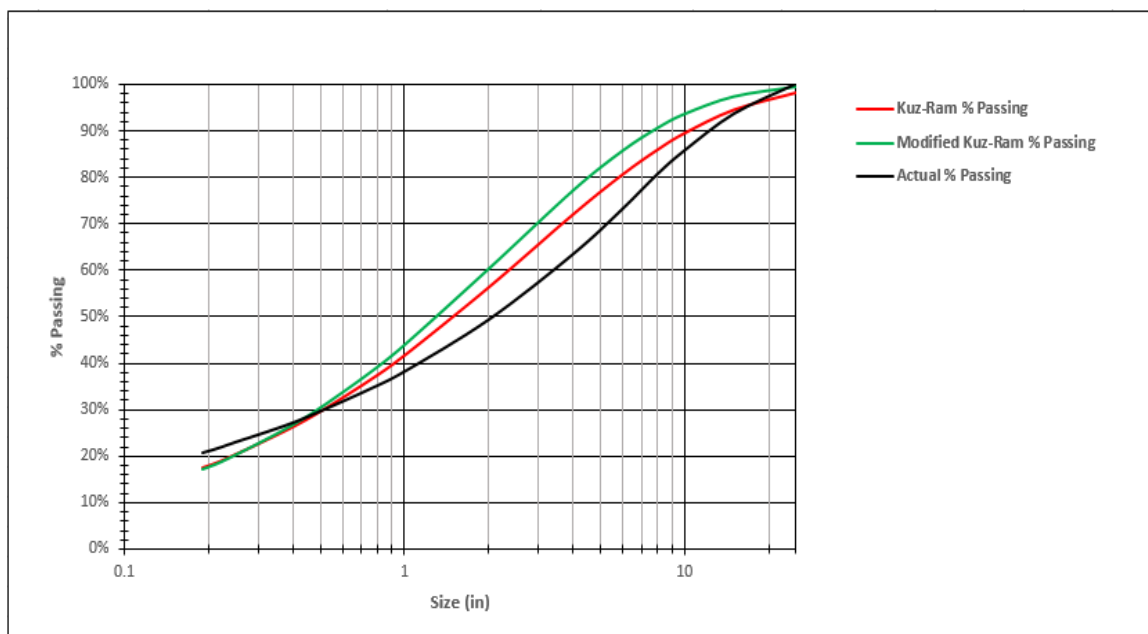


**Figure 19: Actual Size Distribution against Predictive Models for Blast #3054**

**Table VIII: Fragmentation Prediction Summary for Blast #3054**

Fragment Size	Percent Passing (%)		
	Kuz-Ram	Modified Kuz-Ram	Actual Blast from Split (#3054)
Fines (< 0.75 inches)	36.27	37.85	34.51
Average (0.75 inches and 25 inches)	61.83	61.53	65.49
Oversize (>25 inches)	1.9	0.62	0

### 4.3.3. Blast #3056

Fragments from blasting with size less than 0.75 inches are considered as fines. The fines (< 0.75 inches) predicted by the Kuz-Ram and Modified Kuz-Ram models are 29.32% and 30.20% respectively as shown in Table IX. From the actual fragmentation measurement results using Split-Desktop<sup>®</sup>, the fines (< 0.75 inches) produced from this blast were 28.67%. This implies that both the models over predicted the amount of fines produced. The percentage of

over predictions by the Kuz-Ram and Modified Kuz-Ram models are 2.27% and 5.33% respectively.

The material which is within the desired range (0.75 inches and 25 inches) was predicted as 67.41% by Kuz-Ram and 68.52% for Modified Kuz-Ram as presented in Table IX.

Fragments with sizes above 25 inches are considered as Oversize. The oversize (> 25 inches) predictions were 3.27% and 1.28% by Kuz-Ram and Modified Kuz-Ram models respectively. The top size (99.95%) of this blast was 27.20 inches which is above the 25 inches oversize criteria. This indicates over prediction of the oversize material by the fragmentation models with a difference of (< 4%).

The mean fragment sizes predicted by the Kuz-Ram and Modified Kuz-Ram models are 2.16 inches and 1.89 inches respectively. The P50 which represents the actual mean fragmentation of the blast was 3.02 inches. There is therefore under prediction of the mean fragment sizes produced. The percentage under predictions are 28.47% and 37.42% for Kuz-Ram and Modified Kuz-Ram models respectively.

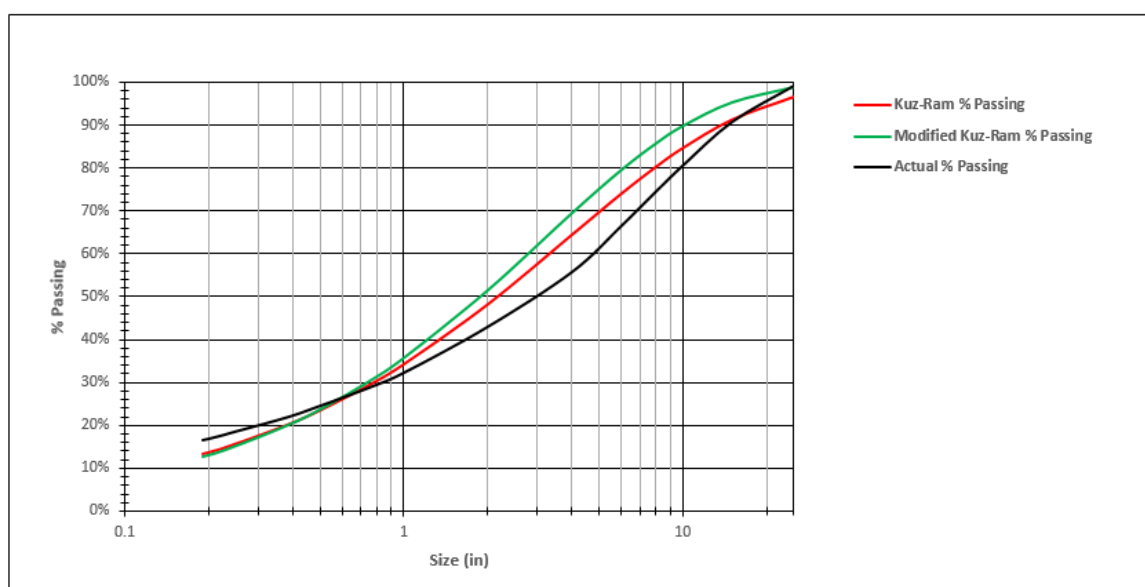


**Figure 20: Actual Size Distribution against Predictive Models for Blast #3056**

**Table IX: Fragmentation Prediction Summary for Blast #3056**

Fragment Size	Percent Passing (%)		
	Kuz-Ram	Modified Kuz-Ram	Actual Blast from Split (#3056)
Fines (< 0.75 inches)	29.32	30.20	28.67
Average (0.75 inches and 25 inches)	67.41	68.52	70.55
Oversize (>25 inches)	3.27	1.28	0.78

#### **4.3.4. Blast #3060**

The Kuz-Ram and Modified Kuz-Ram models predicted 17.88% and 17.66% of fines respectively to be produced from this blast. The actual amount of fines produced however, was approximately 30.01%. The predictions were lower than the actual amount of fines produced. The percentages by which the prediction models was below the actual amount of fines are 40.42% for Kuz Ram and 41.15%% for Modified Kuz-Ram respectively.

The oversize (> 25 inches) predictions were 13.12% and 8.43% by Kuz-Ram and Modified Kuz-Ram models respectively. The top size (99.95%) of this blast was 19.36 inches which is below the 25 inches oversize criteria and hence an insignificant amount of oversize material was produced from the blast. This indicates over prediction of the oversize material by the fragmentation models.

The mean fragment sizes predicted by the Kuz-Ram and Modified Kuz-ram models are 4.97 inches and 4.33 inches respectively. The P50 which represents the actual mean fragmentation of the blast was 2.23 inches. There is therefore over prediction of the mean fragment sizes produced. The percentage over predictions are 122.87% and 94.17% for Kuz-Ram and Modified Kuz-Ram models respectively.

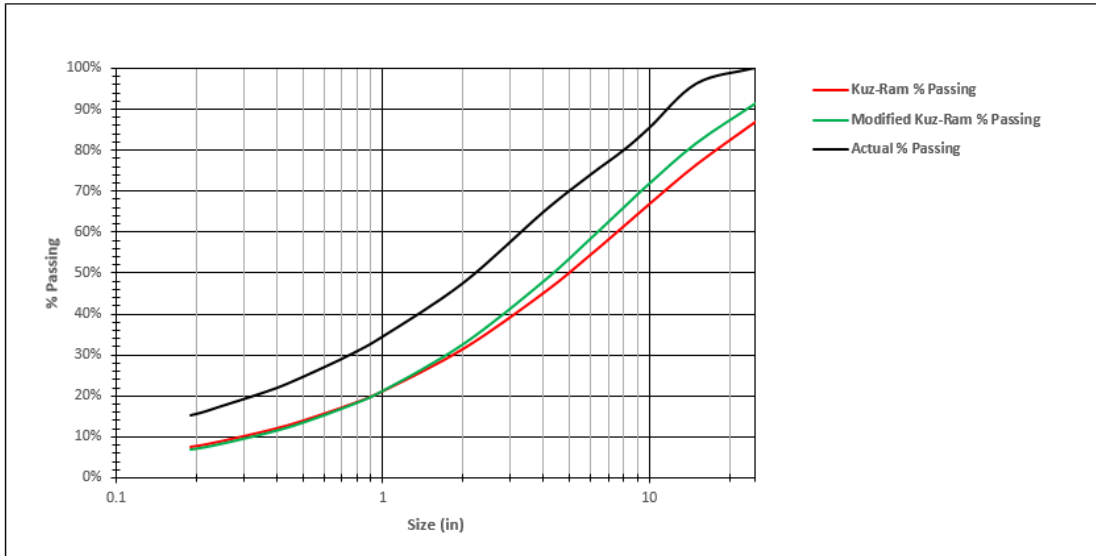


**Figure 21: Actual Size Distribution against Predictive Models for Blast #3060**

**Table X: Fragmentation Prediction Summary for Blast #3060**

Fragment Size	Percent Passing (%)		
	Kuz-Ram	Modified Kuz-Ram	Actual Blast from Split (#3056)
Fines (< 0.75 inches)	17.88	17.66	30.01
Average (0.75 inches and 25 inches)	69	68.52	70.55
Oversize (>25 inches)	13.12	13.82	0

#### 4.3.5. Blast #3062

Fragments from blasting with size less than 0.75 inches are considered as fines. The fines (< 0.75 inches) predicted by the Kuz-Ram and Modified Kuz-Ram models are 19.66% and 19.59% respectively as shown in Table XI. From the actual fragmentation measurement results obtained from Split-Desktop<sup>®</sup>, the fines (< 0.75 inches) produced from this blast were 26.33%. This implies that both the models under predicted the amount of fines produced. The percentage

of under predictions by the Kuz-Ram and Modified Kuz-Ram models are 25.33% and 25.60% respectively.

The material which is within the desired range (0.75 inches and 25 inches) was predicted as 69.87% by Kuz-Ram and 74.17% for Modified Kuz-Ram as presented in Table XI.

The oversize (> 25 inches) predictions were 10.47% and 6.24% by Kuz-Ram and Modified Kuz-Ram models respectively. The top size (99.95%) of this blast was 12.55 inches which is below the 25 inches oversize criteria and hence an insignificant amount of oversize material was produced from the blast. This indicates over prediction of the oversize material by the fragmentation models.

The mean fragment sizes predicted by the Kuz-Ram and Modified Kuz-Ram models are 4.24 inches and 3.69 inches respectively. The P50 which represents the actual mean fragmentation of the blast was 2.07 inches. There is therefore over prediction of the mean fragment sizes produced by the models. The percentage over predictions are 104.83% and 78.26% for Kuz-Ram and Modified Kuz-Ram models respectively.

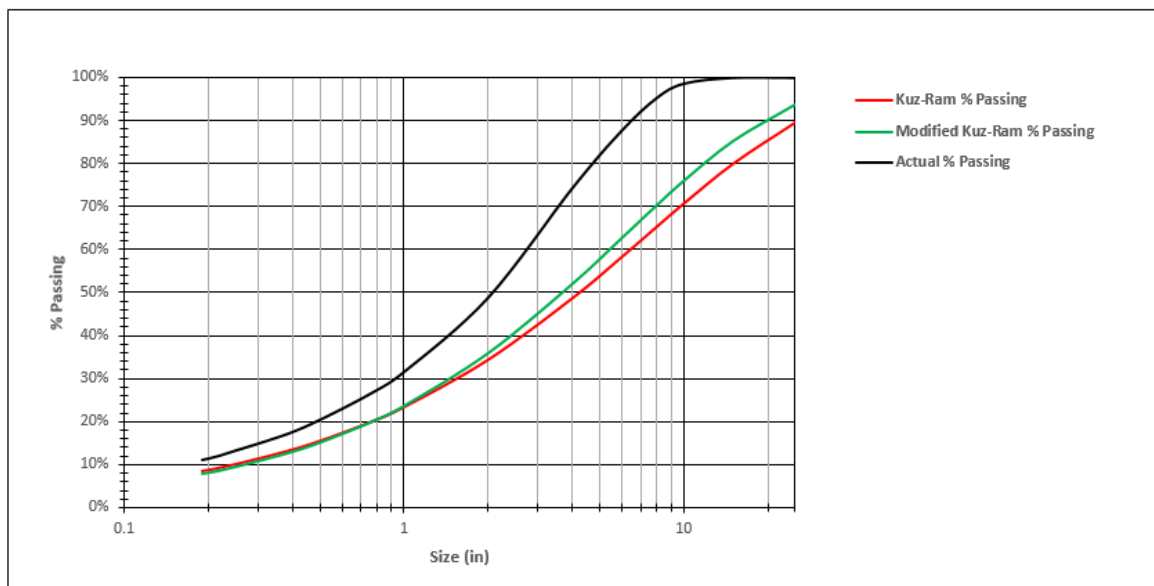


**Figure 22: Actual Size Distribution against Predictive Models for Blast #3062**

**Table XI: Fragmentation Prediction Summary for Blast #3062**

Fragment Size	Percent Passing (%)		
	Kuz-Ram	Modified Kuz-Ram	Actual Blast from Split (#3062)
Fines (< 0.75 inches)	19.66	19.59	26.33
Average (0.75 inches and 25 inches)	69.87	74.17	73.67
Oversize (>25 inches)	10.47	6.24	0

#### **4.3.6. Blast #3063**

The Kuz-Ram and Modified Kuz-Ram models predicted 22.53% and 22.73% of fines (< 0.75 inches) respectively to be produced from this blast. The actual amount produced however, was 25.95%. There is therefore an under prediction of the actual amount of fines from all the models with a difference of 13.18% and 12.41% for the Kuz-Ram and Modified Kuz-Ram models respectively.

The oversize predictions were 7.19% and 3.76% for the Kuz-Ram and Modified Kuz-Ram models respectively. The top size of this blast was 24.97 inches which is below the 25 inches oversize criteria and hence an insignificant amount of oversize material was produced from the blast. This indicates over prediction of the oversize material by the fragmentation models.

The mean fragment sizes predicted by the Kuz-Ram and Modified Kuz-Ram models are 3.36 inches and 2.93 inches. The P50 which represents the actual mean fragmentation was 2.89 inches. All the models over predicted the mean fragmentation. The percentage over predictions are 16.26% and 1.38% for the Kuz-Ram and Modified Kuz-Ram models respectively.

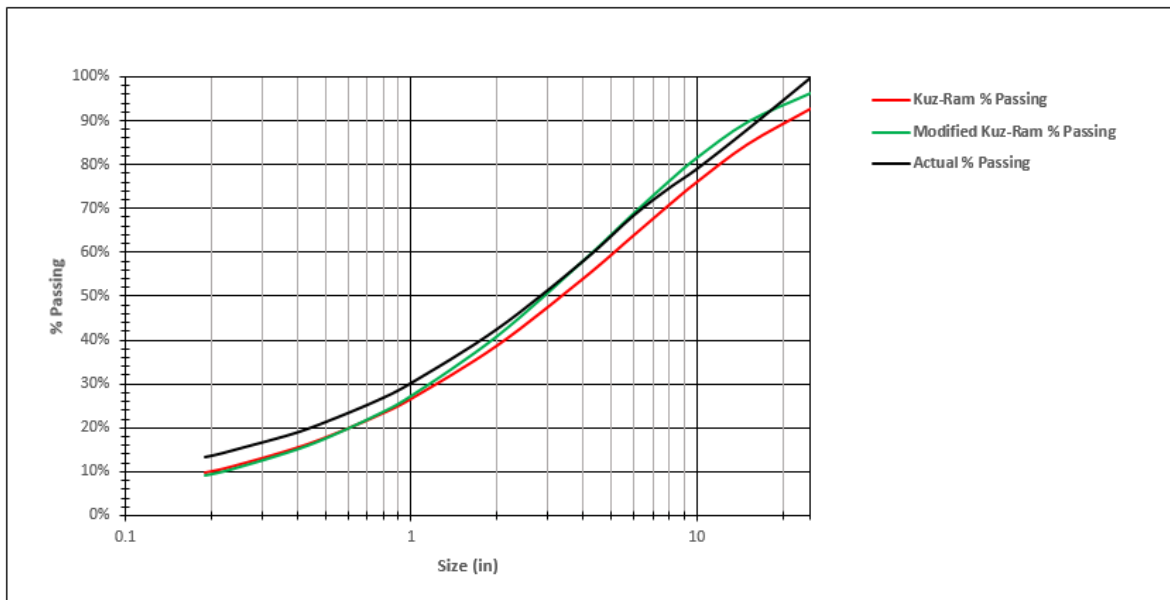


**Figure 23: Actual Size Distribution against Predictive Models for Blast #3063**

**Table XII: Fragmentation Prediction Summary for Blast #3063**

Fragment Size	Percent Passing (%)		
	Kuz-Ram	Modified Kuz-Ram	Actual Blast from Split (#3063)
Fines (< 0.75 inches)	22.53	22.73	25.95
Average (0.75 inches and 25 inches)	70.28	73.51	74.01
Oversize (>25 inches)	7.19	3.76	0.04

#### **4.3.7. Blast #3065**

The Kuz-Ram and Modified Kuz-Ram models predicted 22.28% and 22.45% of fines (< 0.75 inches) respectively to be produced from this blast. The actual amount produced however, was 13.22%. There is therefore an over prediction of the actual amount of fines from all the models a difference of 68.53% and 69.82% for the Kuz-Ram and Modified Kuz-Ram models respectively.

The oversize predictions were 7.43% and 3.93% for the Kuz-Ram and Modified Kuz-Ram models respectively. The top size of this blast was 27.42 inches which is above the 25 inches oversize criteria. This indicates over prediction of the oversize material by the fragmentation models with a difference of (< 9%).

The mean fragment sizes predicted by the Kuz-Ram and Modified Kuz-Ram models are 3.43 inches and 2.99 inches. The P50 which represents the actual mean fragmentation was 4.34 inches. All the models under predicted the mean fragmentation. The percentage under predictions are 20.97% and 31.11% for the Kuz-Ram and Modified Kuz-Ram models respectively.

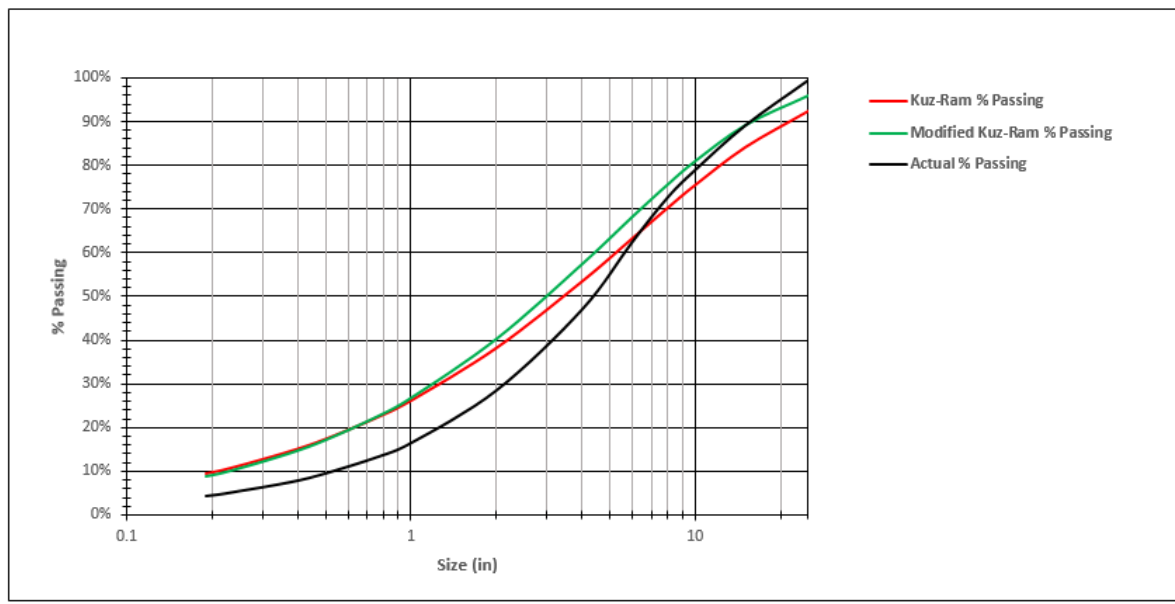


**Figure 24: Actual Size Distribution against Predictive Models for Blast #3065**

**Table XIII: Fragmentation Prediction Summary for Blast #3065**

Fragment Size	Percent Passing (%)		
	Kuz-Ram	Modified Kuz-Ram	Actual Blast from Split (#3065)
Fines (< 0.75 inches)	22.28	22.45	13.22
Average (0.75 inches and 25 inches)	70.29	73.62	86.2
Oversize (>25 inches)	7.43	3.93	0.58

#### **4.3.8. Blast #3067**

The Kuz-Ram and Modified Kuz-Ram models predicted 22.06% and 22.20% of fines respectively to be produced from this blast. The actual amount of fines produced however, was approximately 24.84%. The predictions were lower than the actual amount of fines produced. The percentages of under prediction by the models are 11.19% for Kuz Ram and 10.62% for Modified Kuz-Ram respectively.

The oversize (> 25 inches) predictions were 7.66% and 4.09% by Kuz-Ram and Modified Kuz-Ram models respectively. The top size (99.95%) of this blast was 31.47 inches which is above the 25 inches oversize criteria. This indicates over prediction of the oversize material by the fragmentation models with a difference of (< 8%).

The mean fragment sizes predicted by the Kuz-Ram and Modified Kuz-ram models are 3.49 inches and 3.04 inches respectively. The P50 which represents the actual mean fragmentation of the blast was 3.63 inches. There is therefore under prediction of the mean fragment sizes produced. The percentage under predictions are 3.86% and 16.25% for Kuz-Ram and Modified Kuz-Ram models respectively.

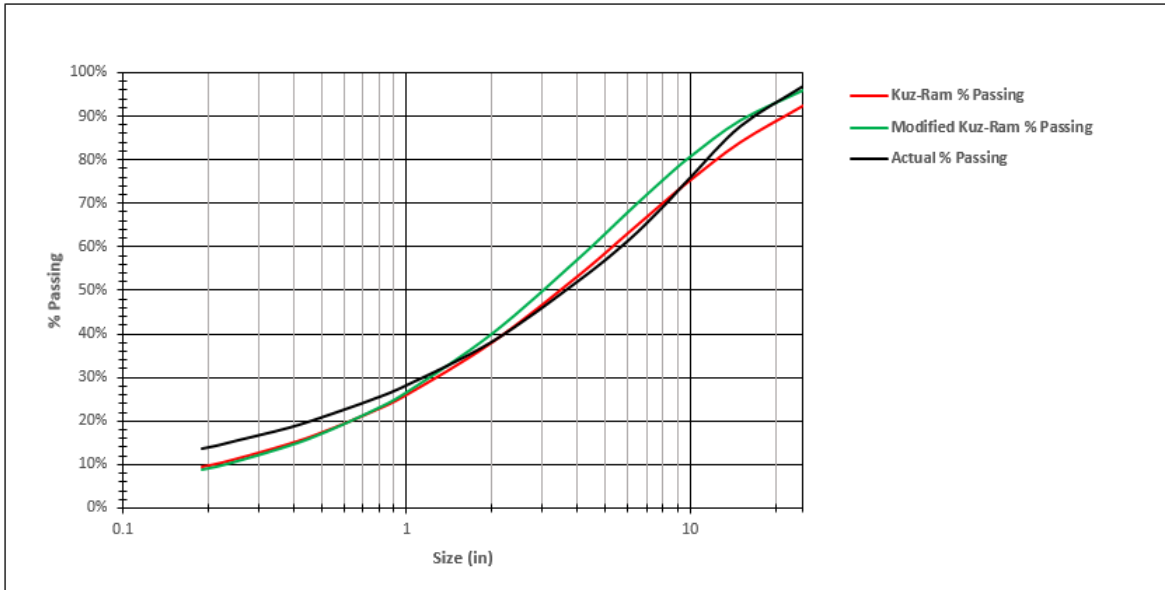


**Figure 25: Actual Size Distribution against Predictive Models for Blast #3067**

**Table XIV: Fragmentation Prediction Summary for Blast #3067**

Fragment Size	Percent Passing (%)		
	Kuz-Ram	Modified Kuz-Ram	Actual Blast from Split (#3067)
Fines (< 0.75 inches)	22.06	22.20	24.84
Average (0.75 inches and 25 inches)	70.28	73.71	72.13
Oversize (>25 inches)	7.66	4.09	3.03

**Table XV: Summary of Predicted Mean Fragment Sizes for the Blasts**

<b>Blast</b>	<b>Mean Fragment Size (inches)</b>		
	<b>Kuz-Ram</b>	<b>Modified Kuz-Ram</b>	<b>Actual Blast from Split</b>
3053	2.05	1.78	1.75
3054	1.50	1.31	2.07
3056	2.16	1.89	3.02
3060	4.97	4.33	2.23
3062	4.24	3.69	2.07
3063	3.36	2.93	2.89
3065	3.43	2.99	4.34
3067	3.49	3.04	3.63

#### **4.4. Determination of Model Performance**

A summary of the results of the Root Mean Square Error (RMSE) computations using the predictions from the models and the fragmentation measurement from image analysis for all the blasts at the Continental pit of the Western US open pit copper mine are shown in Table XVI below. The correlation and regression analysis results are also summarized in Table XVII. The details of the RMSE analyses, correlation and regression analyses are shown in Appendix B and Appendix C, respectively.

Table XVI: Summary of the Estimated RMSE of the Models

Blast	RMSE (%)		Best Predictor compared to Split
	Kuz-Ram	Modified Kuz-Ram	
3053	6.44	6.25	Modified Kuz-Ram
3054	4.27	6.95	Kuz-Ram
3056	4.19	6.92	Kuz-Ram
3060	14.09	11.96	Modified Kuz-Ram
3062	16.56	13.86	Modified Kuz-Ram
3063	3.86	2.87	Modified Kuz-Ram
3065	6.98	6.63	Modified Kuz-Ram
3067	4.34	4.01	Modified Kuz-Ram

Table XVII: Summary of Correlation and Regression Analysis Results for the Models

Blast	Model R (%)		Model R Squared (%)		Best Predictor compared to Split
	Kuz-Ram	Modified Kuz-Ram	Kuz-Ram	Modified Kuz-Ram	
3053	99.5	99.3	99.1	98.6	Modified Kuz-Ram
3054	99.4	98.9	98.8	97.9	Kuz-Ram
3056	99.4	99.7	98.7	98.9	Modified Kuz-Ram
3060	98.9	99.4	98.8	99.4	Modified Kuz-Ram
3062	98.4	98.7	96.9	98.7	Modified Kuz-Ram
3063	99.9	99.8	99.9	99.8	Kuz-Ram
3065	98.9	99.3	97.9	99.3	Modified Kuz-Ram
3067	98.98	99.55	98	99.6	Modified Kuz-Ram

#### 4.5. Model Comparison Discussion

From Table XVI, the Modified Kuz-Ram model had the least RMSE for Blast 3053 (6.25%), Blast 3060 (11.96%), Blast 3062 (13.86%), Blast 3063 (2.87%), Blast 3065 (6.63%) and Blast 3067 (4.01%). The Kuz-Ram model had the least RMSE for Blast 3054 (4.27%) and Blast 3056 (4.19%).

Apart from Blast 3054 and Blast 3056, the Modified Kuz-Ram model performed better than the Kuz-Ram model as it had relatively lower root mean square values. Such that the lower the RMSE value of a model the better its performance. From the Continental pit data and results of RMSE, the Modified Kuz-Ram model had the best prediction performance for all the blasts studied except for Blast 3054 and Blast 3056 for which the Kuz-Ram model had the best performance.

The correlation and regression analysis results confirm those of the root mean square error results. As shown in Table XVII, the Modified Kuz-Ram model had the highest R and  $R^2$  values for six out of the eight blasts considered. This is followed by the Kuz-Ram model having high values of R and  $R^2$  for just two out of the eight blasts considered. Since the Modified Kuz-Ram model had the highest R and  $R^2$  values, it is the model which predicted the actual fragmentation results with the most accuracy and hence it is the best prediction model. The Kuz-Ram model, however can also be used since the R and  $R^2$  values show a strong correlation of the actual fragmentation with the predictions.

## 5. Conclusion and Recommendation

### 5.1. Conclusion

From the study conducted, the following conclusions can be drawn:

- A trend of under estimation was observed in the prediction of the mean fragment sizes for at least five out of the eight blasts considered.
- A general trend of under estimation of the fines ( $< 0.75$  inches) and over estimation of oversize ( $\geq 25$  inches) was observed using the Kuz-Ram and Modified Kuz-Ram models as compared to the Split image analysis obtained on the field.
- The Correlation coefficient, R and Coefficient of determination,  $R^2$  values of all the models were generally high (above 95%). The RMSE for both models were generally low (mostly below 10%). This indicates stronger correlation and good model performance.
- The Modified Kuz-Ram model performed better in the fines regions as the prediction errors were generally less than 10%.
- The average amount of fines produced from the eight blasts studied was 27.62% with an insignificant amount of oversize material less than 5%.
- Among the tested models, the Modified Kuz-Ram model performed best when compared to the blasts studied at the Continental pit of the Western US copper mine.

## 5.2. Recommendations

The following are recommended:

- The Modified Kuz-Ram model should be used for fragmentation prediction and blast optimization at the Western US open pit copper mine.
- Since the results of the predictions from all the models had a strong correlation, they may be used in designing blasts for virgin areas with sufficient knowledge of the rock properties.

## 6. References Cited

- Adebola, J. M., Ajayi, O. D. & Peter, E. O. (2016). Rock fragmentation prediction using Kuz-Ram model. *Journal of Environment and Earth Science*, Department of Minerals and Petroleum Engineering, School of Engineering, Kogi State Polytechnic, Lokoja, Nigeria.
- Anon., (1980). The effect of rock properties on blasting. Part I and II, *Noble Notes*, 26.
- Anon., (2010). *Blasting and Explosives Quick Reference Guide*.
- Anon., (2017). <http://www.austinpowder.com/blasters-zone/formulas-and-calculations/powder-factor/>
- Ash, R. L. (1968). The design of blasting rounds. Chapter 7.3, E.P. Pfleider (ed.), *Surface Mining*, AIME, New York, 373-397.
- Bamford, T. (2016). A real-time analysis of rock fragmentation using UAV technology. University of Toronto Institute of Aerospace Studies, Toronto, Canada.
- Barnston, A. G. (1992). Correspondence among the Correlation, RMSE and Heidke Forecast verification measures; Refinement of the Heidke Score, *Journal of weather and forecasting*, Vol. 7, 699-709.
- Bergman, P. (2005). Optimization of fragmentation and comminution at Boliden Mineral, Aitik Operation, Lulea University of Technology, Department of Civil and Environmental Engineering Division of Rock Engineering, Unpublished MSc. Thesis Report, Sweden, 20.
- Bhandari, S. (1997). *Engineering rock blasting operations*. A.A. Balkema, Rotterdam, Brookfield, 375.
- Choudhary, B. S. & Gupta, A. (2012). A comparative study on fragmentation measurement techniques. *Mining Engineers' Journal*, Mining Engineers' Association of India, Vol. 14, 16-24.
- Cunningham, C. (1983). The Kuz-Ram model for prediction of fragmentation blasting. 1<sup>st</sup> International Symposium Rock Fragmentation by Blasting, Lulea, Sweden.
- Cunningham, C. V. B. (1987). Fragmentation estimations and the Kuz-Ram model – four years on. *Proceedings of the Second International Symposium on Rock Fragmentation by Blasting*, Keystone, Colorado, 475-487.

- Faramarzi, F., Mansouri, H. & Ebrahimi Farsangi, M. A. (2013). A rock engineering systems based model to predict rock fragmentation by blasting, *International Journal of Rock Mechanics & Mining Science* 60, 82-94.
- Gheibie, S. Aghababaei, H., Hosienie, S. H. & Pourrahimian, Y. (2009). Modified Kuz-Ram fragmentation model and its use at the Sungun Copper Mine. *International Journal of Rock Mechanics & Mining Sciences*, Vol. 46, 967-973.
- Girdner, K., Kemeny, J., Srikant, A. & McGill, R. (1996). The split system for analyzing the size distribution of fragmented rock, *Proceedings of the Fragblast-5 workshop on Management of Blast Fragmentation*, A.A. Balkema, Montreal, Quebec, Canada, 101-108.
- Gregory, C. E. (1973). *Explosives for North American Engineers*. Trans Tech Publications, Clausthal, 273.
- Gustafsson, R. (1981). Blasting technique. *Dynamite Noble*, 81-89, 121-127.
- Hemphill, G. B. (1981). *Blasting operations*. McGraw-Hill, Inc., New York, 258.
- Higgins, M., Bobo, T., Girdner, K., Kemeny, J. & Seppala, V. (1999). Integrated software tools and methodology for optimization of blast fragmentation. *Proceedings of the Twenty-Fifth Annual Conference on Explosives and Blasting Technique*, Nashville, Tennessee, USA, Volume II, 355-368.
- Jimeno, C. L., Jimeno, E. L., & Carcedo, F. J. A. (1995). *Drilling and blasting of rocks*, A.A. Balkema, Rotterdam, Netherlands.
- Johnson, C. E. (2014). *Fragmentation analysis in the dynamic stress wave collision regions in bench blasting*. Unpublished PhD Thesis Report, University of Kentucky, USA, 158.
- Kemeny, J., Girdner, K. & Bobo, T. (1999). New advances in digital image analysis software to quantify the size distribution of fragmented rock. *MINNBLAST 99*, 27-43.
- Konya, C. J. and Walter, E. J. (1990). *Surface blasting design*. Prentice Hall Publishing, Englewood, New Jersey, USA.
- Konya, C. J., Skidmore, D. R., & Otuonye, F. O. (1981). *Control of airblast and excessive ground vibrations from blasting by efficient stemming*. US Department of Interior, Office of Surface Mining.
- Kuznetsov, V. M. (1973). The mean diameter of fragments formed by blasting. *J Min Sci*; 9, 144-148.

- Lilly, P. A. (1986). An empirical method of assessing rock mass blastability. Proceedings, Large Open Pit Mining Conference (J. R. Davidson, ed.), the AusIMM, Parkville, Victoria.
- Marinos, P. & Hoek, E. (2011). Estimating the geotechnical properties of heterogeneous rock masses such as flysch. Bull Engineering, Geology and the Environment.
- Mishra, A. (2009). Design of surface blast – A computational approach. Unpublished Bachelor of Technology Project Report, National Institute of Technology, Rourkeda, India, 11.
- Monjezi, M. & Rezaei, M. (2011). Developing a new fuzzy model to predict burden from rock geomechanical properties. Journal of Expert Systems with Applications, Vol. 38, 9266-9273.
- Muhammed, A. R. (2009). The effect of fragmentation specification on blasting cost. Unpublished MSc. Thesis Report, Queen's University, Kingston, Ontario, Canada, 192.
- Online Mining Exam (2018). Explosives and Blasting – Part 5. Retrieved from <https://onlineminingexam.wordpress.com/2015/12/11/explosives-and-blasting-part-5/>
- Prof. Pathak, K. (2014). Introduction to drilling technology for surface mining. Department of Mining Engineering, IIT, kharagpur-721302.
- Vasileosis, D. (2008). Fragmentation analysis of optimized blasting rounds in the Aitik Mine – Effect of specific charge. Unpublished Master's Thesis Report, Lulea University of Technology, Sweden.
- Willmott, C. J. & Matsuura, K. (2005). Advantages of the mean absolute error (MAE) over the root mean square error (RMSE) in assessing average model performance. , Vol. 30, 79-82.

## 7. Appendix A: Actual Fragmentation distribution and Predictive Models Results.

Table XVIII: Size Distribution Results for Blast #3053.

Size (in)	Kuz-Ram % Passing	Modified Kuz-Ram % Passing	Actual % Passing from Split
0	0.00%	0.00%	0.00%
0.08	8.01%	7.33%	17.94%
0.19	13.66%	13.13%	23.73%
0.25	16.11%	15.73%	26.09%
0.38	20.61%	20.59%	29.80%
0.5	24.13%	24.44%	32.73%
0.75	30.12%	31.20%	37.45%
1	35.21%	36.80%	41.34%
2	49.45%	52.83%	52.22%
4	65.78%	70.78%	65.94%
6	75.27%	80.64%	76.94%
8	81.47%	86.66%	85.31%
10	85.77%	90.57%	90.44%
15	92.12%	95.72%	96.58%
25	97.12%	98.92%	100.00%

**Table XIX: Size Distribution Results for Blast #3054.**

<b>Size (in)</b>	<b>Kuz-Ram % Passing</b>	<b>Modified Kuz-Ram % Passing</b>	<b>Actual % Passing from Split</b>
0	0.00%	0.00%	0.00%
0.08	10.64%	9.95%	15.35%
0.19	17.50%	17.14%	20.88%
0.25	20.39%	20.26%	23.18%
0.38	25.59%	25.95%	26.84%
0.5	29.56%	30.34%	29.78%
0.75	36.27%	37.85%	34.51%
1	41.64%	43.88%	38.31%
2	56.29%	60.27%	49.45%
4	71.97%	77.11%	63.50%
6	80.51%	85.62%	73.19%
8	85.84%	90.52%	80.67%
10	89.40%	93.54%	85.73%
15	94.42%	97.28%	93.60%
25	98.10%	99.38%	100.00%

**Table XX: Size Distribution Results for Blast #3056.**

<b>Size (in)</b>	<b>Kuz-Ram % Passing</b>	<b>Modified Kuz-Ram % Passing</b>	<b>Actual % Passing from Split</b>
0	0.00%	0.00%	0.00%
0.08	7.74%	7.05%	11.63%
0.19	13.21%	12.66%	16.41%
0.25	15.58%	15.17%	18.44%
0.38	19.96%	19.88%	21.71%
0.5	23.38%	23.62%	24.39%
0.75	29.32%	30.20%	28.67%
1	34.21%	35.67%	32.16%
2	48.22%	51.45%	42.91%
4	64.46%	69.37%	55.68%
6	74.02%	79.37%	66.39%
8	80.33%	85.59%	74.48%
10	84.76%	89.67%	80.60%
15	91.38%	95.17%	90.77%
25	96.73%	98.72%	99.22%

**Table XXI: Size Distribution Results for Blast #3060.**

<b>Size (in)</b>	<b>Kuz-Ram % Passing</b>	<b>Modified Kuz-Ram % Passing</b>	<b>Actual % Passing from Split</b>
0	0.00%	0.00%	0.00%
0.08	4.35%	3.76%	10.05%
0.19	7.60%	6.93%	15.30%
0.25	9.05%	8.39%	17.62%
0.38	11.78%	11.19%	21.46%
0.5	13.97%	13.48%	24.65%
0.75	17.88%	17.66%	30.01%
1	21.22%	21.29%	34.54%
2	31.50%	32.69%	47.57%
4	45.12%	48.03%	64.88%
6	54.43%	58.46%	73.93%
8	61.39%	66.12%	79.94%
10	66.85%	71.99%	85.42%
15	76.45%	81.87%	96.17%
25	86.88%	91.57%	100.00%

**Table XXII: Size Distribution Results for Blast #3062.**

<b>Size (in)</b>	<b>Kuz-Ram % Passing</b>	<b>Modified Kuz-Ram % Passing</b>	<b>Actual % Passing from Split</b>
0	0.00%	0.00%	0.00%
0.08	4.82%	4.21%	6.55%
0.19	8.40%	7.74%	11.10%
0.25	10.00%	9.36%	13.27%
0.38	13.00%	12.46%	17.07%
0.5	15.39%	14.99%	20.42%
0.75	19.66%	19.59%	26.33%
1	23.28%	23.55%	31.57%
2	34.32%	35.86%	48.88%
4	48.66%	52.01%	74.38%
6	58.24%	62.67%	87.72%
8	65.27%	70.30%	95.30%
10	70.68%	76.01%	98.63
15	79.94%	85.27%	100.00%
25	89.53%	93.76%	100.00%

**Table XXIII: Size Distribution Results for Blast #3063.**

<b>Size (in)</b>	<b>Kuz-Ram % Passing</b>	<b>Modified Kuz-Ram % Passing</b>	<b>Actual % Passing from Split</b>
0	0.00%	0.00%	0.00%
0.08	5.60%	4.96%	8.83%
0.19	9.73%	9.08%	13.19%
0.25	11.57%	10.97%	15.13%
0.38	14.99%	14.57%	18.39%
0.5	17.71%	17.48%	21.17%
0.75	22.53%	22.73%	25.95%
1	26.60%	27.22%	30.13%
2	38.76%	40.86%	42.49%
4	54.05%	58.04%	58.05%
6	63.89%	68.82%	68.44%
8	70.87%	76.21%	74.72%
10	76.09%	81.51%	79.11%
15	84.65%	89.62%	88.10%
25	92.81%	96.24%	99.96%

**Table XXIV: Size Distribution Results for Blast #3065.**

<b>Size (in)</b>	<b>Kuz-Ram % Passing</b>	<b>Modified Kuz-Ram % Passing</b>	<b>Actual % Passing from Split</b>
0	0.00%	0.00%	0.00%
0.08	5.53%	4.89%	2.28%
0.19	9.62%	8.96%	4.46%
0.25	11.43%	10.83%	5.60%
0.38	14.82%	14.38%	7.68%
0.5	17.51%	17.26%	9.62%
0.75	22.28%	22.45%	13.22%
1	26.31%	26.90%	16.56%
2	38.38%	40.43%	28.60%
4	53.60%	57.53%	47.07%
6	63.42%	68.32%	62.46%
8	70.41%	75.73%	72.65%
10	75.65%	81.08%	78.92%
15	84.28%	89.29%	89.07%
25	92.57%	96.07%	99.42%

**Table XXV: Size Distribution Results for Blast #3067.**

<b>Size (in)</b>	<b>Kuz-Ram % Passing</b>	<b>Modified Kuz-Ram % Passing</b>	<b>Actual % Passing from Split</b>
0	0.00%	0.00%	0.00%
0.08	5.47%	4.83%	9.51%
0.19	9.51%	8.86%	13.65%
0.25	11.30%	10.70%	15.44%
0.38	14.66%	14.21%	18.36%
0.5	17.32%	17.06%	20.80%
0.75	22.06%	22.20%	24.84%
1	26.05%	26.61%	28.22%
2	38.03%	40.04%	38.22%
4	53.19%	57.07%	52.04%
6	62.99%	67.85%	61.31%
8	69.99%	75.30%	69.21%
10	75.25%	80.68%	75.97%
15	83.94%	88.99%	87.72%
25	92.34%	95.91%	96.97%

## 8. Appendix B: Root Mean Square Error Results for the Predictive Models.

Table XXVI: RMSE results for Blast #3053.

RMSE for C-South 5560-3053							
Size (inches)	Kuz-Ram Model	Modified Kuz-Ram Model	Actual from Split	Error (Kuz-Ram)	Error (Modified Kuz-Ram)	Squared Error (Kuz-Ram)	Squared Error (Modified Kuz-Ram)
0	0.000	0.000	0.000	0.000	0.000	0.000	0.000
0.08	0.080	0.073	0.179	-0.099	-0.106	0.010	0.011
0.19	0.137	0.131	0.237	-0.101	-0.106	0.010	0.011
0.25	0.161	0.157	0.261	-0.100	-0.104	0.010	0.011
0.38	0.206	0.206	0.298	-0.092	-0.092	0.008	0.008
0.5	0.241	0.244	0.327	-0.086	-0.083	0.007	0.007
0.75	0.302	0.312	0.375	-0.072	-0.063	0.005	0.004
1	0.352	0.368	0.413	-0.061	-0.045	0.004	0.002
2	0.495	0.528	0.522	-0.028	0.006	0.001	0.000
4	0.658	0.708	0.659	-0.002	0.048	0.000	0.002
6	0.753	0.806	0.769	-0.017	0.037	0.000	0.001
8	0.815	0.867	0.853	-0.038	0.014	0.001	0.000
10	0.858	0.906	0.904	-0.047	0.001	0.002	0.000
15	0.921	0.957	0.965	-0.044	-0.008	0.002	0.000
25	0.971	0.989	1.000	-0.029	-0.011	0.001	0.000

Table XXVII: RMSE results for Blast #3054.

RMSE for C-South 5560-3054							
Size (inches)	Kuz-Ram Model	Modified Kuz-Ram Model	Actual from Split	Error (Kuz-Ram)	Error (Modified Kuz-Ram)	Squared Error (Kuz-Ram)	Squared Error (Modified Kuz-Ram)
0	0.000	0.000	0.000	0.000	0.000	0.000	0.000
0.08	0.106	0.099	0.154	-0.047	-0.054	0.002	0.003
0.19	0.175	0.171	0.209	-0.034	-0.037	0.001	0.001
0.25	0.204	0.203	0.232	-0.028	-0.029	0.001	0.001
0.38	0.256	0.259	0.268	-0.013	-0.009	0.000	0.000
0.5	0.296	0.303	0.298	-0.002	0.006	0.000	0.000
0.75	0.363	0.379	0.345	0.018	0.033	0.000	0.001
1	0.416	0.439	0.383	0.033	0.056	0.001	0.003
2	0.563	0.603	0.495	0.068	0.108	0.005	0.012
4	0.720	0.771	0.635	0.085	0.136	0.007	0.019
6	0.805	0.856	0.732	0.073	0.124	0.005	0.015
8	0.858	0.905	0.807	0.052	0.098	0.003	0.010
10	0.894	0.935	0.857	0.037	0.078	0.001	0.006
15	0.944	0.973	0.936	0.008	0.037	0.000	0.001
25	0.981	0.994	1.000	-0.019	-0.006	0.000	0.000

Table XXVIII: RMSE results for Blast #3056.

RMSE for C-South 5560-3056							
Size (inches)	Kuz-Ram Model	Modified Kuz-Ram Model	Actual from Split	Error (Kuz-Ram)	Error (Modified Kuz-Ram)	Squared Error (Kuz-Ram)	Squared Error (Modified Kuz-Ram)
0	0.000	0.000	0.000	0.000	0.000	0.000	0.000
0.08	0.077	0.071	0.116	-0.039	-0.046	0.002	0.002
0.19	0.132	0.127	0.164	-0.032	-0.037	0.001	0.001
0.25	0.156	0.152	0.184	-0.029	-0.033	0.001	0.001
0.38	0.200	0.199	0.217	-0.017	-0.018	0.000	0.000
0.5	0.234	0.236	0.244	-0.010	-0.008	0.000	0.000
0.75	0.293	0.302	0.287	0.006	0.015	0.000	0.000
1	0.342	0.357	0.322	0.020	0.035	0.000	0.001
2	0.482	0.514	0.429	0.053	0.085	0.003	0.007
4	0.645	0.694	0.557	0.088	0.137	0.008	0.019
6	0.740	0.794	0.664	0.076	0.130	0.006	0.017
8	0.803	0.856	0.745	0.059	0.111	0.003	0.012
10	0.848	0.897	0.806	0.042	0.091	0.002	0.008
15	0.914	0.952	0.908	0.006	0.044	0.000	0.002
25	0.967	0.987	0.992	-0.025	-0.005	0.001	0.000

Table XXIX: RMSE results for Blast #3060.

RMSE for C-East 5280-3060							
Size (inches)	Kuz-Ram Model	Modified Kuz-Ram Model	Actual from Split	Error (Kuz-Ram)	Error (Modified Kuz-Ram)	Squared Error (Kuz-Ram)	Squared Error (Modified Kuz-Ram)
0	0.000	0.000	0.000	0.000	0.000	0.000	0.000
0.08	0.043	0.038	0.101	-0.057	-0.063	0.003	0.004
0.19	0.076	0.069	0.153	-0.077	-0.084	0.006	0.007
0.25	0.090	0.084	0.176	-0.086	-0.092	0.007	0.009
0.38	0.118	0.112	0.215	-0.097	-0.103	0.009	0.011
0.5	0.140	0.135	0.247	-0.107	-0.112	0.011	0.012
0.75	0.179	0.177	0.300	-0.121	-0.123	0.015	0.015
1	0.212	0.213	0.345	-0.133	-0.132	0.018	0.018
2	0.315	0.327	0.476	-0.161	-0.149	0.026	0.022
4	0.451	0.480	0.649	-0.198	-0.168	0.039	0.028
6	0.544	0.585	0.739	-0.195	-0.155	0.038	0.024
8	0.614	0.661	0.799	-0.185	-0.138	0.034	0.019
10	0.668	0.720	0.854	-0.186	-0.134	0.034	0.018
15	0.764	0.819	0.962	-0.197	-0.143	0.039	0.020
25	0.869	0.916	1.000	-0.131	-0.084	0.017	0.007

Table XXX: RMSE results for Blast #3062.

RMSE for C-East 5280-3062							
Size (inches)	Kuz-Ram Model	Modified Kuz-Ram Model	Actual from Split	Error (Kuz-Ram)	Error (Modified Kuz-Ram)	Squared Error (Kuz-Ram)	Squared Error (Modified Kuz-Ram)
0	0.000	0.000	0.000	0.000	0.000	0.000	0.000
0.08	0.048	0.042	0.066	-0.017	-0.023	0.000	0.001
0.19	0.084	0.077	0.111	-0.027	-0.034	0.001	0.001
0.25	0.100	0.094	0.133	-0.033	-0.039	0.001	0.002
0.38	0.130	0.125	0.171	-0.041	-0.046	0.002	0.002
0.5	0.154	0.150	0.204	-0.050	-0.054	0.003	0.003
0.75	0.197	0.196	0.263	-0.067	-0.067	0.004	0.005
1	0.233	0.236	0.316	-0.083	-0.080	0.007	0.006
2	0.343	0.359	0.489	-0.146	-0.130	0.021	0.017
4	0.487	0.520	0.744	-0.257	-0.224	0.066	0.050
6	0.582	0.627	0.877	-0.295	-0.250	0.087	0.063
8	0.653	0.703	0.953	-0.300	-0.250	0.090	0.062
10	0.707	0.760	0.986	-0.280	-0.226	0.078	0.051
15	0.799	0.853	1.000	-0.201	-0.147	0.040	0.022
25	0.895	0.938	1.000	-0.105	-0.062	0.011	0.004

Table XXXI: RMSE results for Blast #3063.

RMSE for C-East 5280-3063							
Size (inches)	Kuz-Ram Model	Modified Kuz-Ram Model	Actual from Split	Error (Kuz-Ram)	Error (Modified Kuz-Ram)	Squared Error (Kuz-Ram)	Squared Error (Modified Kuz-Ram)
0	0.000	0.000	0.000	0.000	0.000	0.000	0.000
0.08	0.056	0.050	0.088	-0.032	-0.039	0.001	0.001
0.19	0.097	0.091	0.132	-0.035	-0.041	0.001	0.002
0.25	0.116	0.110	0.151	-0.036	-0.042	0.001	0.002
0.38	0.150	0.146	0.184	-0.034	-0.038	0.001	0.001
0.5	0.177	0.175	0.212	-0.035	-0.037	0.001	0.001
0.75	0.225	0.227	0.260	-0.034	-0.032	0.001	0.001
1	0.266	0.272	0.301	-0.035	-0.029	0.001	0.001
2	0.388	0.409	0.425	-0.037	-0.016	0.001	0.000
4	0.541	0.580	0.581	-0.040	0.000	0.002	0.000
6	0.639	0.688	0.684	-0.046	0.004	0.002	0.000
8	0.709	0.762	0.747	-0.038	0.015	0.001	0.000
10	0.761	0.815	0.791	-0.030	0.024	0.001	0.001
15	0.846	0.896	0.881	-0.035	0.015	0.001	0.000
25	0.928	0.962	1.000	-0.071	-0.037	0.005	0.001

Table XXXII: RMSE results for Blast #3065.

RMSE for C-East 5280-3065							
Size (inches)	Kuz-Ram Model	Modified Kuz-Ram Model	Actual from Split	Error (Kuz-Ram)	Error (Modified Kuz-Ram)	Squared Error (Kuz-Ram)	Squared Error (Modified Kuz-Ram)
0	0.000	0.000	0.000	0.000	0.000	0.000	0.000
0.08	0.055	0.049	0.023	0.032	0.026	0.001	0.001
0.19	0.096	0.090	0.045	0.052	0.045	0.003	0.002
0.25	0.114	0.108	0.056	0.058	0.052	0.003	0.003
0.38	0.148	0.144	0.077	0.071	0.067	0.005	0.004
0.5	0.175	0.173	0.096	0.079	0.076	0.006	0.006
0.75	0.223	0.225	0.132	0.091	0.092	0.008	0.009
1	0.263	0.269	0.166	0.097	0.103	0.010	0.011
2	0.384	0.404	0.286	0.098	0.118	0.010	0.014
4	0.536	0.575	0.471	0.065	0.105	0.004	0.011
6	0.634	0.683	0.625	0.010	0.059	0.000	0.003
8	0.604	0.757	0.727	-0.122	0.031	0.015	0.001
10	0.757	0.811	0.789	-0.033	0.022	0.001	0.000
15	0.843	0.893	0.891	-0.048	0.002	0.002	0.000
25	0.926	0.961	0.994	-0.069	-0.034	0.005	0.001

Table XXXIII: RMSE results for Blast #3067.

RMSE for C-East 5280-3067							
Size (inches)	Kuz-Ram Model	Modified Kuz-Ram Model	Actual from Split	Error (Kuz-Ram)	Error (Modified Kuz-Ram)	Squared Error (Kuz-Ram)	Squared Error (Modified Kuz-Ram)
0	0.000	0.000	0.000	0.000	0.00	0.000	0.000
0.08	0.055	0.048	0.095	-0.040	-0.047	0.002	0.002
0.19	0.095	0.089	0.137	-0.041	-0.048	0.002	0.002
0.25	0.113	0.107	0.154	-0.041	-0.047	0.002	0.002
0.38	0.147	0.142	0.184	-0.037	-0.041	0.001	0.002
0.5	0.173	0.171	0.208	-0.035	-0.037	0.001	0.001
0.75	0.221	0.222	0.248	-0.028	-0.026	0.001	0.001
1	0.360	0.266	0.282	0.078	-0.016	0.006	0.000
2	0.480	0.400	0.382	0.098	0.018	0.010	0.000
4	0.532	0.517	0.520	0.011	0.050	0.000	0.003
6	0.630	0.679	0.613	0.017	0.065	0.000	0.004
8	0.700	0.753	0.692	0.008	0.061	0.000	0.004
10	0.753	0.807	0.760	-0.007	0.047	0.000	0.002
15	0.839	0.890	0.877	-0.038	0.013	0.001	0.000
25	0.923	0.959	0.970	-0.046	-0.011	0.002	0.000

## 9. Appendix C: Correlation and Regression Analysis Results.

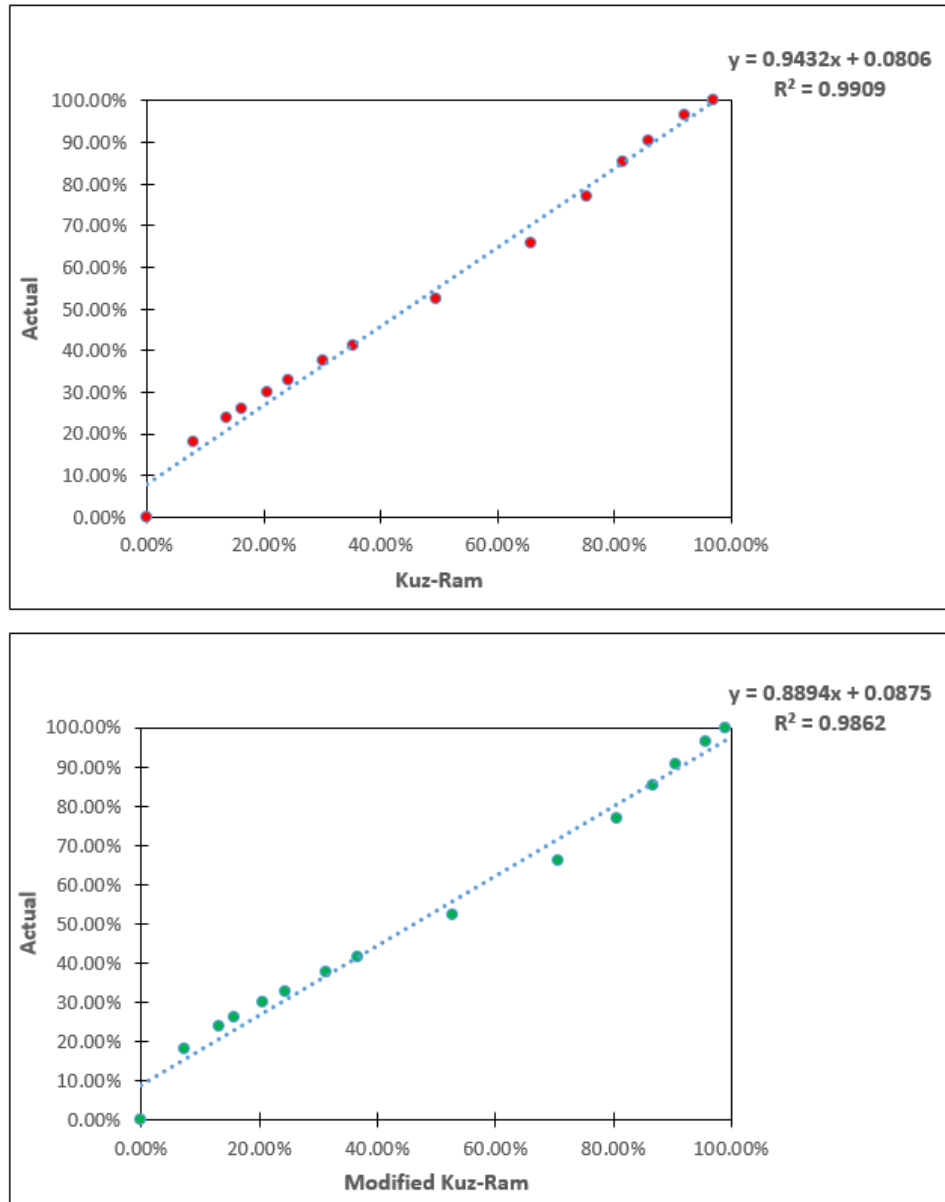


Figure 26: Correlation between Actual Predicted Fragmentation Results for Blast #3053.

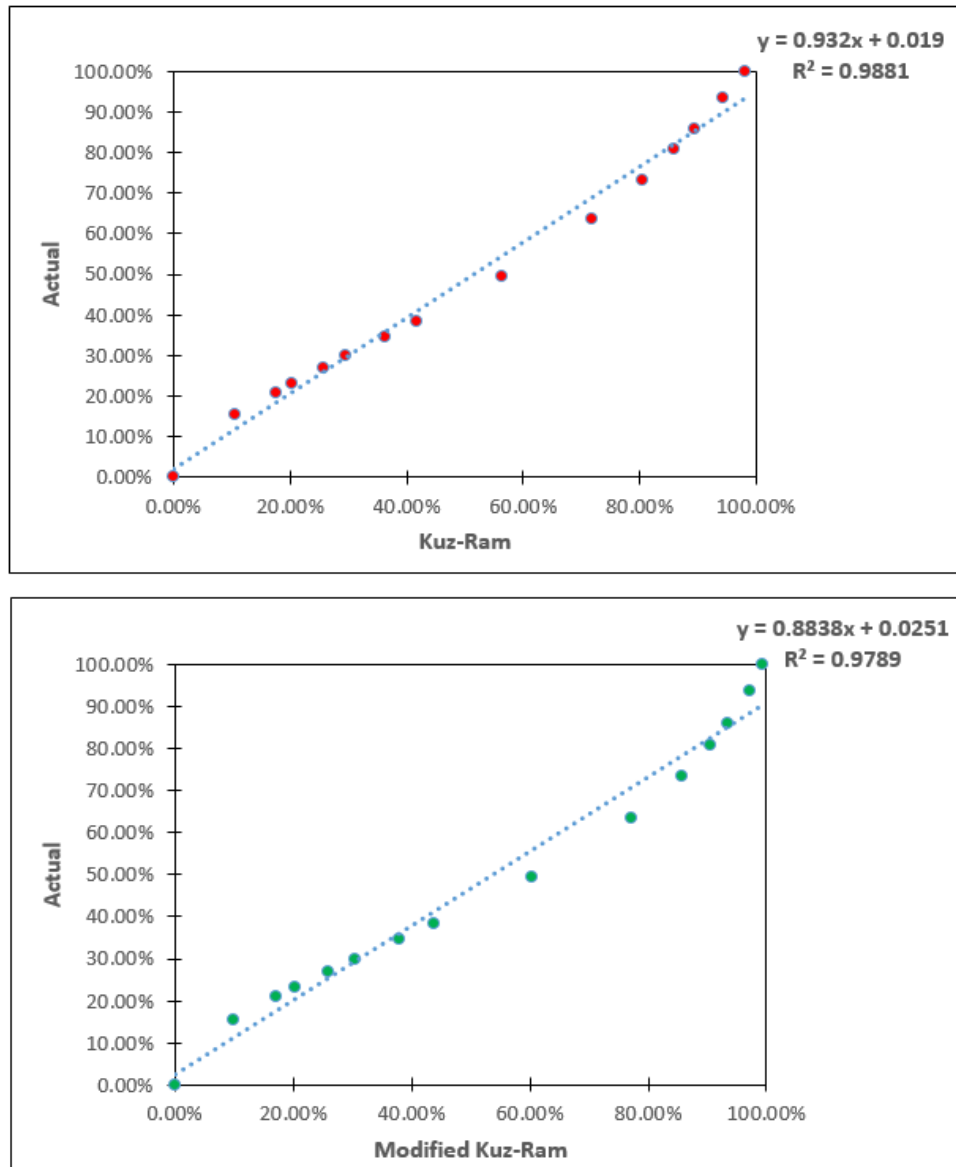


Figure 27: Correlation between Actual Predicted Fragmentation Results for Blast #3054.

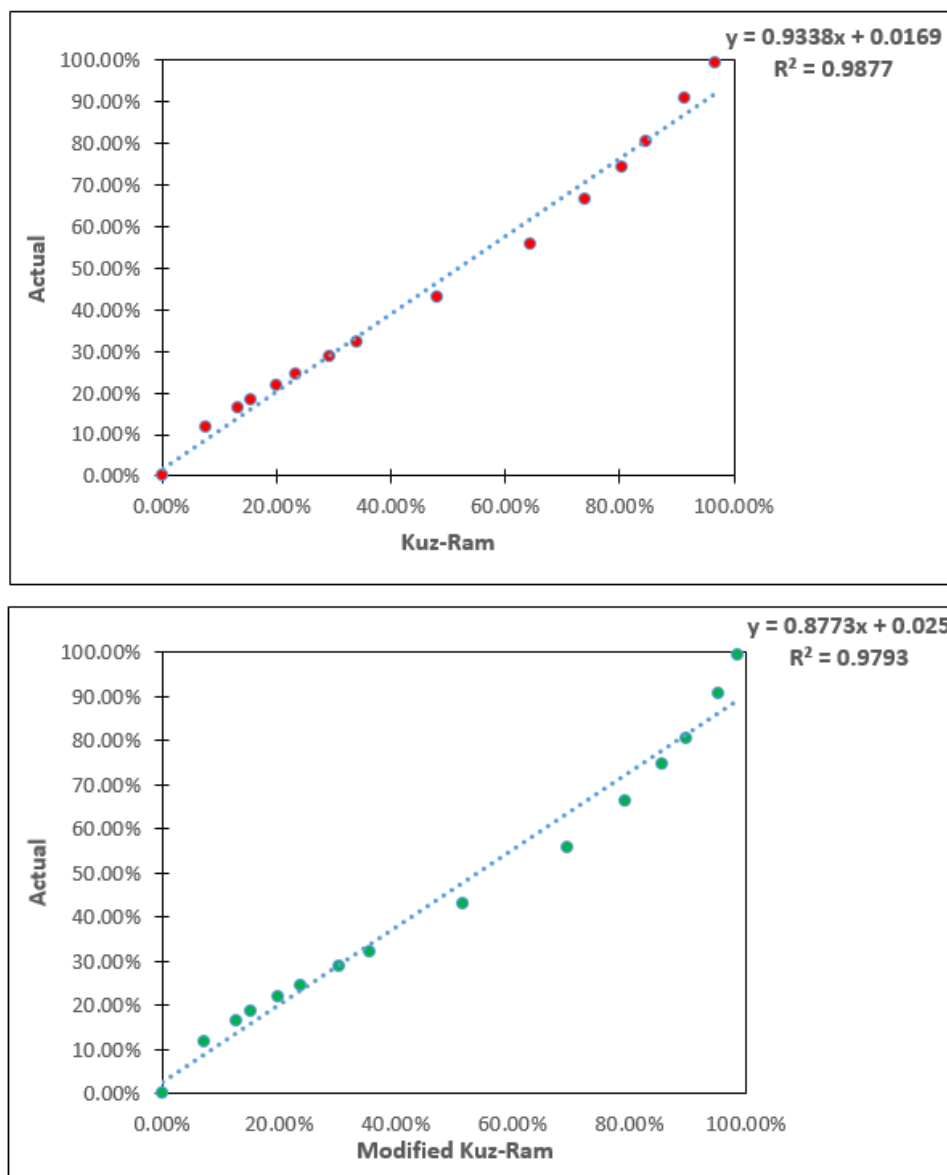


Figure 28: Correlation between Actual Predicted Fragmentation Results for Blast #3056.

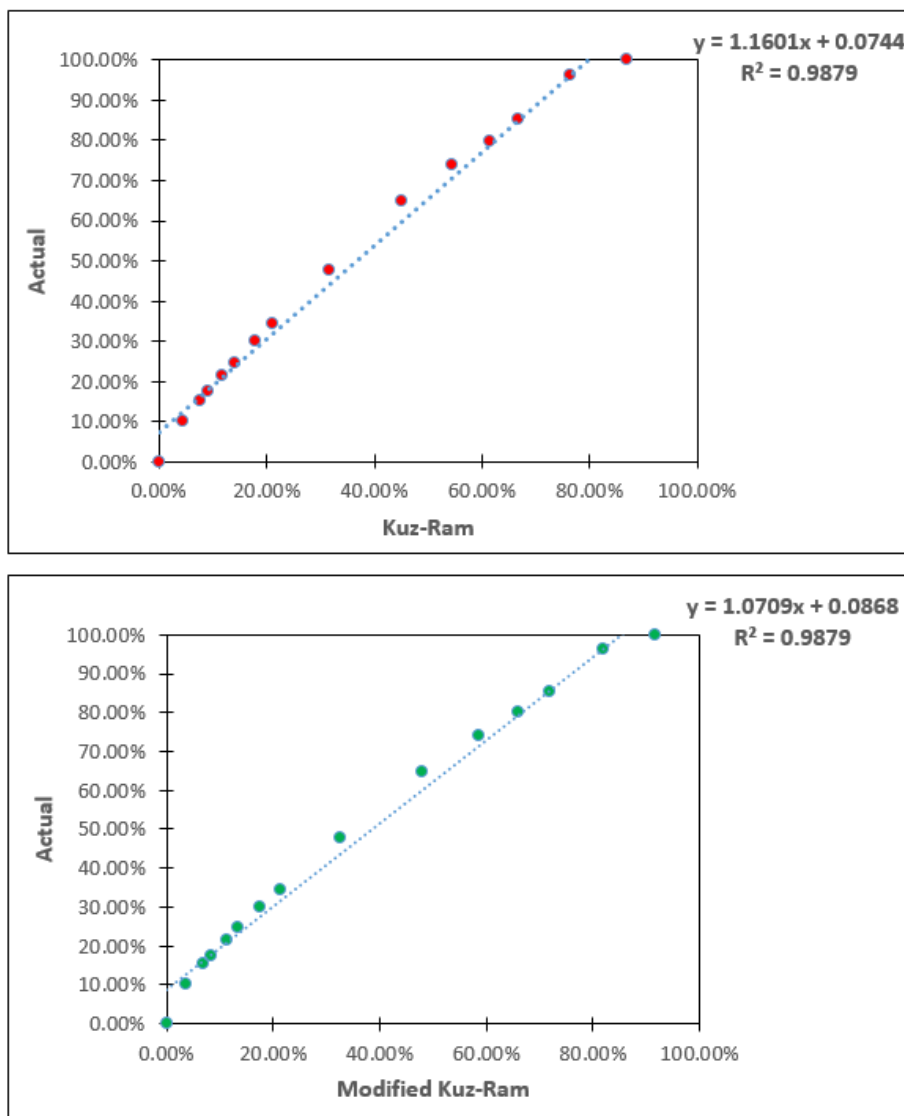


Figure 29: Correlation between Actual Predicted Fragmentation Results for Blast #3060.

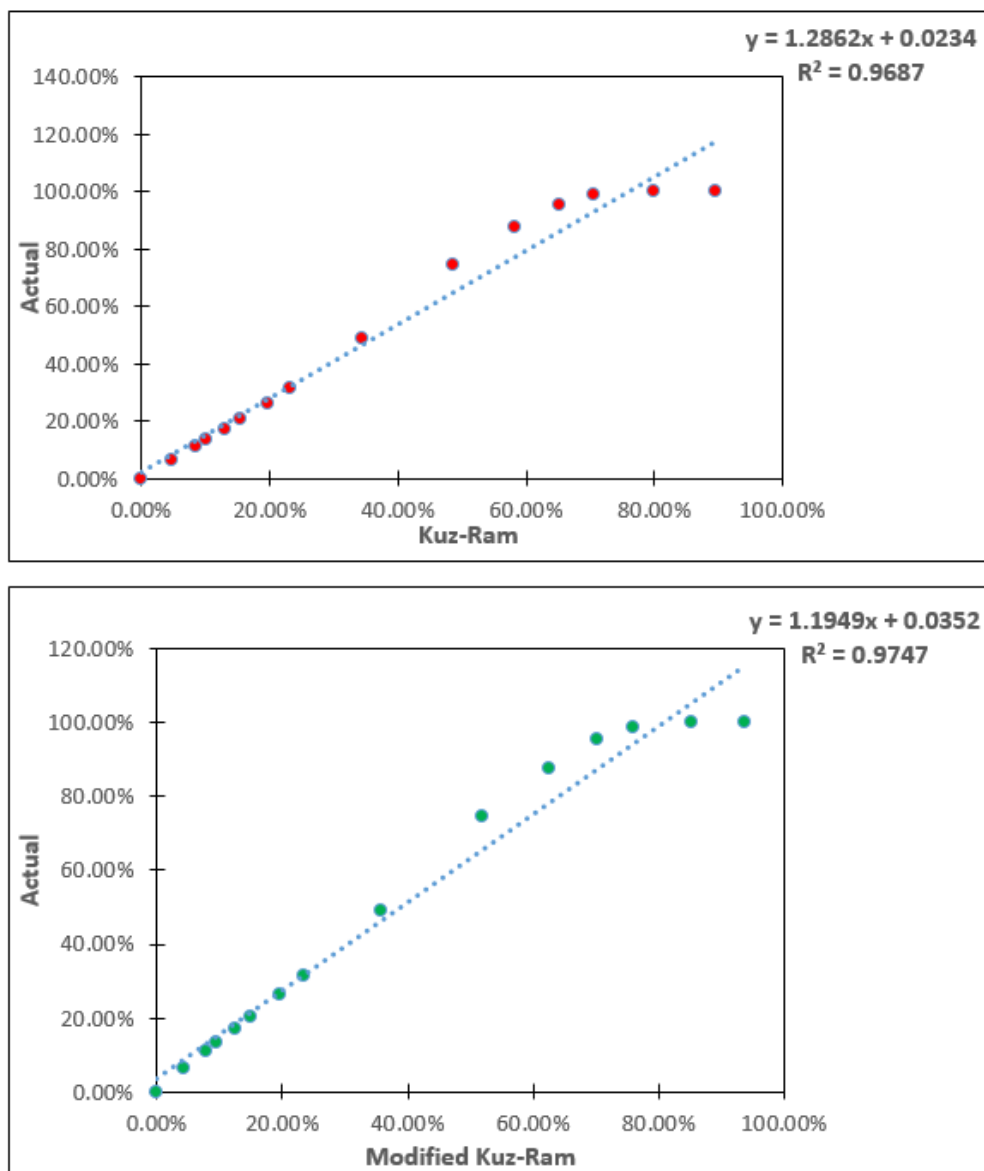


Figure 30: Correlation between Actual Predicted Fragmentation Results for Blast #3062.

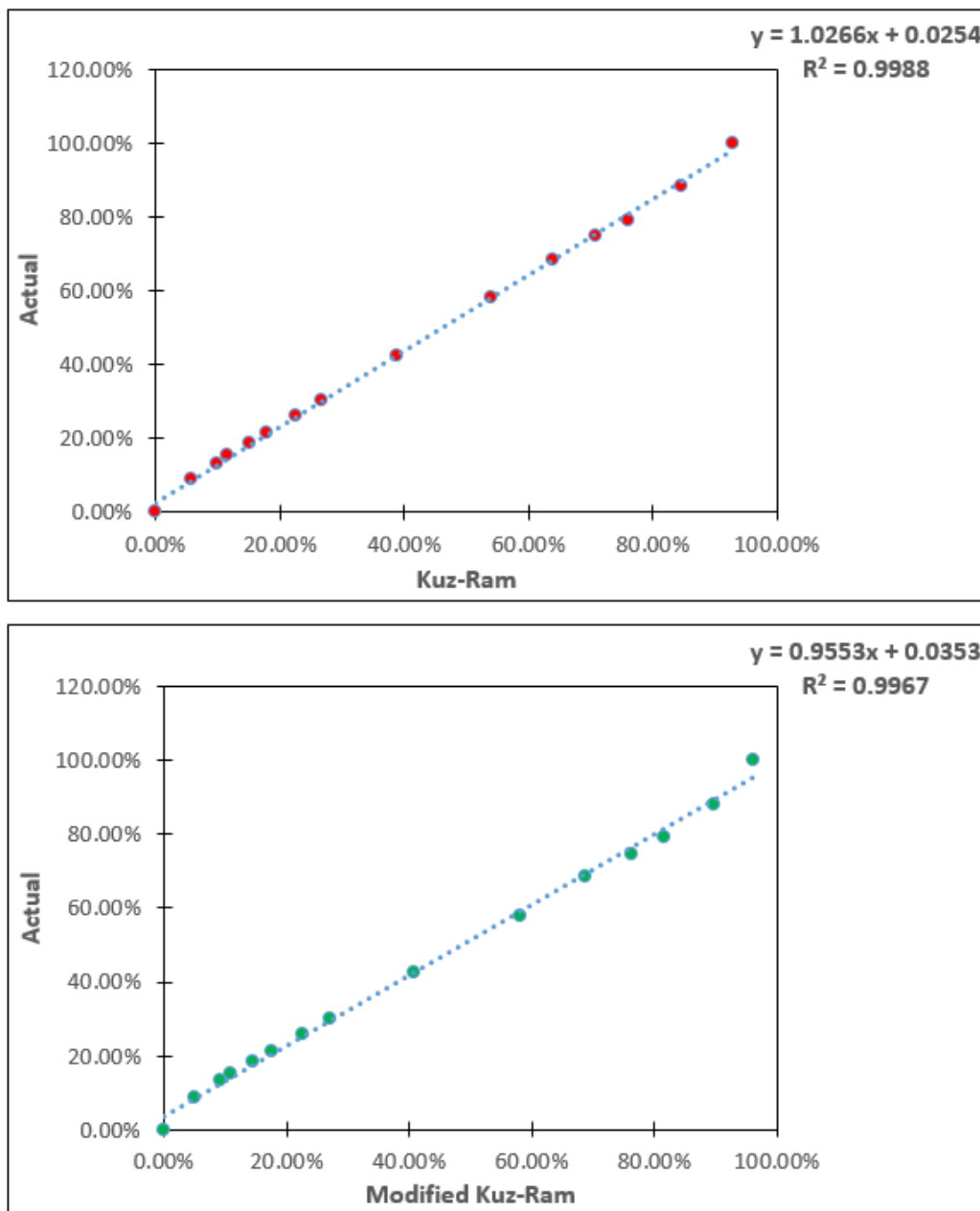


Figure 31: Correlation between Actual Predicted Fragmentation Results for Blast #3063.

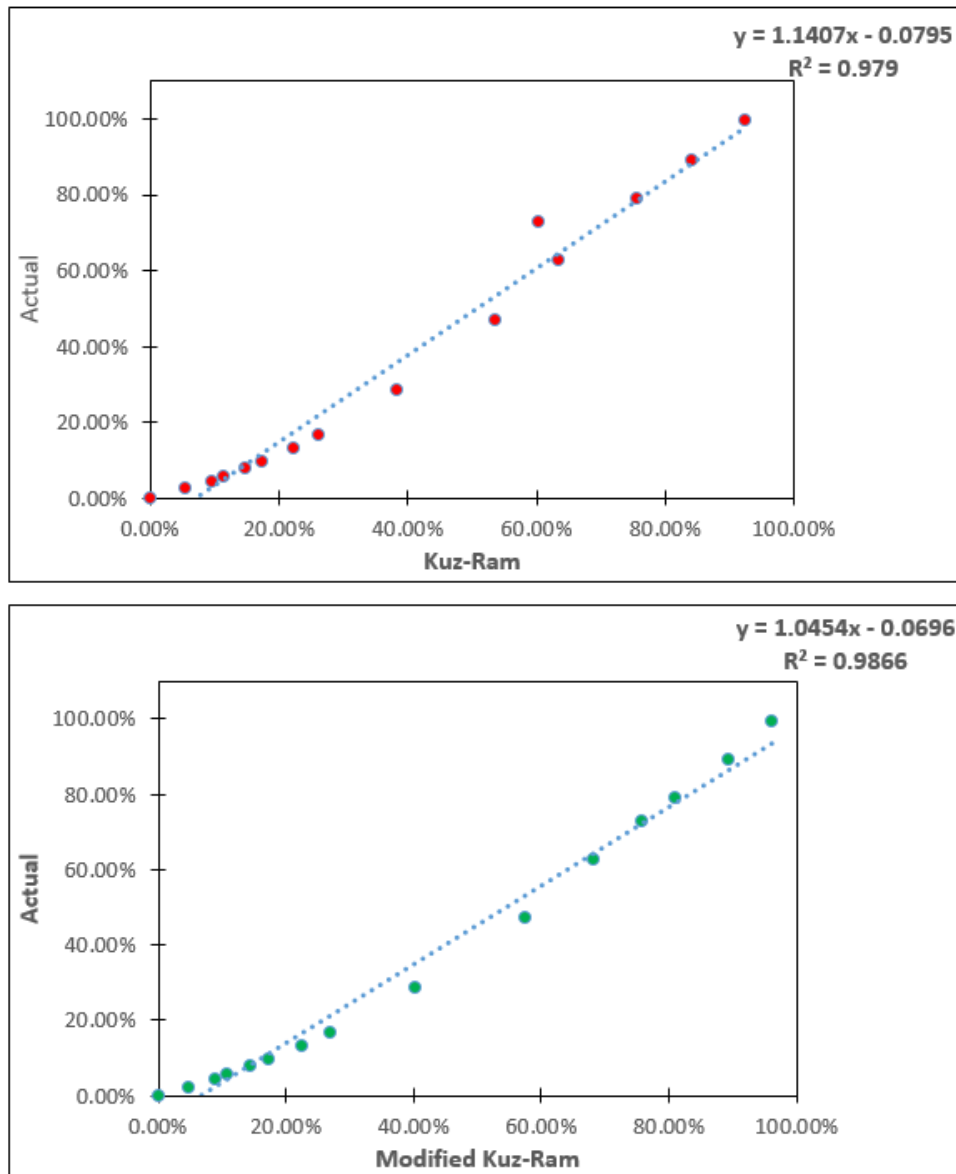


Figure 32: Correlation between Actual Predicted Fragmentation Results for Blast #3065.

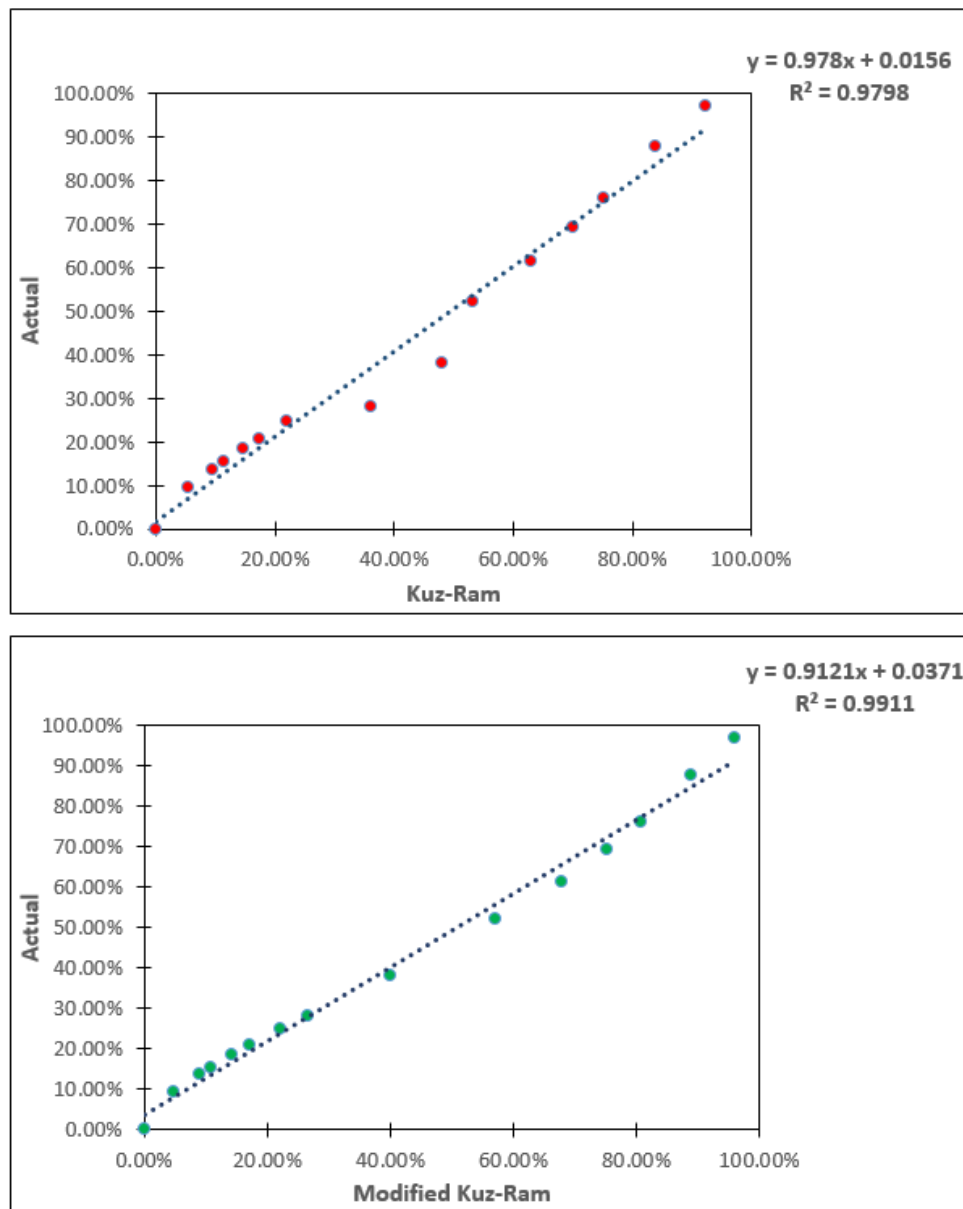


Figure 33: Correlation between Actual Predicted Fragmentation Results for Blast #3067.

## SIGNATURE PAGE

This is to certify that the thesis prepared by Joel Edem Kwaku Gadikor entitled "Optimization of Drilling and Blasting Practices at a Western US Open Pit Mine" has been examined and approved for acceptance by the Department of Mining Engineering, Montana Tech of The University of Montana, on this 27th day of April, 2018.



---

Scott Rosenthal, P.E, Assistant Professor and Department Head  
Department of Mining Engineering  
Chair, Examination Committee



---

Chris Roos, P.E, Assistant Professor  
Department of Mining Engineering  
Member, Examination Committee



---

Das Avimanyu, PhD, Associate Professor  
Department of Metallurgical & Materials Engineering  
Member, Examination Committee